Sheffield Hallam University

Design of a Multi-Complex Disturbance Generator Using Virtual Instrumentation for Power Quality Monitoring Research

ABDULLAH, Saud, USMAN, Adil, KHAN, Muhammad Umar, AZIZ, Sumair, KHAN, Muhammad Faisal Nadeem and AKMAL, Muhammad <http://orcid.org/0000-0002-3498-4146>

Available from Sheffield Hallam University Research Archive (SHURA) at:

https://shura.shu.ac.uk/37646/

This document is the Published Version [VoR]

Citation:

ABDULLAH, Saud, USMAN, Adil, KHAN, Muhammad Umar, AZIZ, Sumair, KHAN, Muhammad Faisal Nadeem and AKMAL, Muhammad (2026). Design of a Multi-Complex Disturbance Generator Using Virtual Instrumentation for Power Quality Monitoring Research. Energy Science & Engineering, 14 (10), 4700-4721. [Article]

Copyright and re-use policy

See http://shura.shu.ac.uk/information.html

Sheffield Hallam University Research Archive
http://shura.shu.ac.uk

Energy Science & Engineering

WILEY

ORIGINAL ARTICLE OPEN ACCESS

Design of a Multi-Complex Disturbance Generator Using Virtual Instrumentation for Power Quality Monitoring Research

Abdullah Saud[1] | Adil Usman[1] | Muhammad Umar Khan[2] | Sumair Aziz[2] | Muhammad Faisal Nadeem Khan[3] | Muhammad Akmal[4]

[1]Department of Electronics Engineering, University of Engineering and Technology Taxila, Taxila, Pakistan | [2]Human-Centred Technology Research Centre, Faculty of Science and Technology, University of Canberra, Canberra, Australian Capital Territory, Australia | [3]Department of Electrical Engineering, University of Engineering and Technology Taxila, Taxila, Pakistan | [4]School of Engineering and Built Environment, Sheffield Hallam University, Sheffield, UK

Correspondence: Muhammad Akmal (m.akmal@shu.ac.uk)

Received: 26 January 2026 | **Revised:** 24 June 2026 | **Accepted:** 26 June 2026

Keywords: data acquisition card | IEEE standards | measurement uncertainty | power quality disturbance (PQD) generator | Virtual instrument (VI)

ABSTRACT

The reliability and feasibility of power quality disturbance (PQD) classification methods pivot their performance in a real-world electrical environment. This demands an instrument that can generate real-time PQD voltage signals for investigating the performance of a PQD detection algorithm in practical scenarios. This research presents a PQD generator capable of generating fifteen real-time disturbance events using mathematical models specified by the IEEE standard for monitoring Power Quality (PQ). The proposed design is based on the concept of virtual instrumentation, comprising two parts: the first one is LabVIEW software platform for defining the disturbance parameters and synthesizing user-defined simulated PQD signal, and the second one is MyDAQ a data acquisition card from National Instruments (NI)) for real-time voltage signal generation. The virtual instrument (VI) designed in LabVIEW provides a unique option of inducing real-world electrical conditions like Additive White Gaussian Noise (AWGN) and harmonic distortion to PQD events in real-time. The reliability of the proposed instrument is evaluated by measuring the uncertainty in voltage and frequency of the generated PQD waveforms in accordance with the instructions provided by ISO-guide to the expression of uncertainty in measurement.

1 | Introduction

With the increasing use of distributed generation and power electronic devices, various types of single and multi-complex power quality disturbances (PQDs) may occur simultaneously. PQDs cause malfunctioning and damage to the electrical load connected to the network. This necessitates to adopt counter-measures [1–3]. Recognizing the adverse effects on electronic loads, the mitigation of PQDs has emerged as a crucial subject [4–8]. Before initiating the protection systems like dynamic voltage restorer (DVR) and distribution static compensator (D-STATCOM), it is mandatory to detect and classify these PQ disturbances [9–11]. Researchers are actively involved in designing efficient PQD detection and recognition algorithms for PQ monitoring [3, 12]. The majority of the PQD detection and classification schemes presented previously are simulation-based studies. The detection algorithms presented in these research works are trained and tested using PQD signal data sets that are generated through software simulations [13–19]. For that purpose, they utilize the mathematical models of PQ disturbances provided by IEEE standard 1159 to generate these signal data sets [11, 20–26]. Most of the cases, the researchers have performed the experimentation using ideal voltage signal obtained through these mathematical equations. Some of the

This is an open access article under the terms of the Creative Commons Attribution License, which permits use, distribution and reproduction in any medium, provided the original work is properly cited.

© 2026 The Author(s). *Energy Science & Engineering* published by Society of Chemical Industry and John Wiley & Sons Ltd.

researchers have also presented open-source software for producing data sets of different PQ signals. MATLAB software has been used to create graphical user interface (GUI). Despite these efforts, the PQ signal data sets synthesized through software simulations lack incorporation of real-world scenarios [27].

The reliability and feasibility of PQD classification methods depend on their performance in a real-world electrical environment, where noise is commonly superimposed on the actual voltage signal, and waveform distortion can occur due to harmonic distortion in the line. A detection scheme is ranked to be feasible and realizable in a practical PQD monitoring system if its performance remains robust in the presence of such electrical conditions. Consequently, it is mandatory to train the algorithm on real signals and to confirm the regulated high-end performance before implementing it on hardware for PQD monitoring systems. This necessitates a departure from relying on synthetic PQD signal data sets and emphasizes the requirement for a dedicated PQD generation device capable of producing authentic signals. Such a device should also provide the flexibility of introducing various electrical conditions in the clean signal, enabling rigorous testing of PQD detection algorithms, validating their authenticity, and verifying their performance.

Addressing the design challenges associated with sophisticated PQ generation devices, the importance of virtual instruments has gained attention, particularly in computer-based PQ measurement and monitoring systems. Regardless of that, the existing literature presents a limited number of PQD generation methods and devices. A design of PQD generator aligned with the European standard EN50160 was presented in 2017. Proposed design consists of two parts, disturbance parameters setting module based on virtual instrumentation software (LabVIEW), a data acquisition card interface, and the design of the output power amplifier. Emphasis was placed on amplifier design to scale the output voltage level of the data acquisition card to the nominal line voltage (230 V), facilitating the generation of disturbance signals for testing power quality instruments and algorithms [28].

Another virtual generator using LabVIEW was introduced in 2020 that aimed to produce real-time PQDs. It has two modes of operation, continuous mode in which desired disturbance was generated on a trigger input, and pre-defined mode, which implements the exact definition of events. The LabVIEW program was implemented on data acquisition device-based hardware. However, the hardware presented in the study could generate only 12 PQDs. Moreover, the research lacked information about measurement uncertainty, which is a critical aspect for signal-generating instruments [29]. A PQD generator was proposed for the generation of voltage sag, swell, and interruption. The design comprised of solid-state relays and dimmer-stat-I. Solid-state relays are used to select the type of PQD and dimmer stat controlled by microcontroller 89C51 was employed to change voltage levels and duration of disturbance. The presented PQD generator is imitated to generating only four single disturbances, lacking information about the sampling frequency, and the produced signals are clean and ideal [30].

Researchers have also presented a method for obtaining real events generated from real-time digital simulator (RTDS) under various operating scenarios and noise levels. RSCAD software was utilized for simulated signal generation and for GUI. The hardware component involved interfacing multiple digital signal processors to generate only nine real-time disturbance signals [31]. In a study, a virtual instrument-based platform was proposed for the generation and detection of transient PQDs. LabVIEW software-oriented generator gave transient disturbance signals according to the standard IEEE1159-1995. It is noteworthy that this method could generate only nine types of disturbance events [32]. Authors have also introduced three-phase PQD generators that were able to generate only seven types of PQ signals. PQ standard equations, control parameters, and design of GUI were implemented on LabVIEW. The real-time PQ voltage signals were generated through a data acquisition board NI PCI 6713. The generator could add Gaussian noise to the PQ signals. This PQ signal generation setup is not user-friendly due to its reliance on PCI slot [33]. In research, electronic circuits were presented to generate some of the power quality distortions, including voltage sag, swell, outage, harmonic distortion, notches, and voltage unbalance. Simulations of these circuits confirmed the accuracy of the generated disturbances, making it particularly suitable for testing power devices such as UPS, DVR, SSTS, etc [34]. Some electrical circuit-based hardware has also been presented in various studies. The examples of these PQD generating circuits are impedance switching-based PQ generator, back-to-back converter circuit, transformer-based generator, and AC chopper-based generator. Although these PQ generator circuits are reliable, their scope is limited to only three types of PQ disturbances, that is, sag, swell, and interruption [10, 35, 36].

Based on the above review, the specific shortcomings of existing PQD generation research can be summarized as follows. First, many PQD detection and classification studies still rely on software-generated data sets or ideal mathematical waveforms based on standard PQD models [13–27], which do not sufficiently represent practical operating conditions such as noise contamination and harmonic distortion. Second, several reported PQD generators are limited to a small number of disturbance classes, including 12 disturbances in [29], four single disturbances in [30], nine disturbance signals in [31, 32], seven PQ signals in [33], and mainly sag, swell, and interruption in circuit-based generators [10, 35, 36]. Therefore, these approaches do not adequately support the flexible generation of single and multi-complex PQD events. Third, some available hardware-based generators either do not report measurement uncertainty [29], lack detailed sampling-frequency information and generate clean ideal waveforms only [30], or focus on simulation/circuit-level verification rather than flexible signal-generation instrumentation [34]. This weakens confidence in their use as validated signal-generating instruments. Fourth, some reported platforms rely on less portable or less user-friendly hardware arrangements, such as PCI-based acquisition systems [33] or application-specific circuit configurations [10, 34–36], limiting their suitability for flexible laboratory use. These limitations indicate the need for a portable, user-configurable, virtual-instrumentation-based PQD generator that can produce both single and multi-complex disturbances, incorporate user-defined AWGN and harmonic distortion, and

20500505, 2026, 10, Downloaded from https://scijournals.onlinelibrary.wiley.com/doi/10.1002/ese3.70602 by Sheffield Hallam University, Wiley Online Library on [14/10/2026]. See the Terms and Conditions (https://onlinelibrary.wiley.com/terms-and-conditions) on Wiley Online Library for rules of use; OA articles are governed by the applicable Creative Commons License

provide measurement uncertainty analysis for generator-level validation.

To address these shortcomings, this study presents a LabVIEW-MyDAQ-based PQD generator with controllable disturbance parameters, real-time waveform generation, user-defined AWGN and harmonic distortion insertion, and voltage/frequency uncertainty analysis. The main contributions are as follows:

1. Designing of PQD generator, capable of generating 15 single and multi-complex PQ disturbance signals in accordance with IEEE standard.
2. Device is equipped with the options of adding user-defined total harmonic distortion (THD) and additive white Gaussian noise (AWGN) in PQD signal to emulate real-world electrical conditions.
3. A user-friendly GUI is designed to offer complete control of all the disturbance model parameters.
4. A detailed study for the measurement of device's uncertainty is presented pursuing the guidelines suggested in the "ISO Guide to the Expression of Uncertainty in Measurement" that highlights authenticity of proposed design.
5. The PQ signals generated by the proposed instrument undergo evaluation using a PQD recognition algorithm presented in a recent study, demonstrating remarkably accurate results that validate the generator.

2 | Proposed Design of PQD Generator

2.1 | Overview of PQD Generator

The proposed design of the PQD generator for the generation of single and multi-complex PQ disturbances is based on the concept of virtual instrumentation. Figure 1 shows the system block diagram of the signal generation scheme implemented in the proposed PQD generator. There are five primary blocks of the PQD generator: (1) General Parameter Setting block, (2) PQD Selection & Disturbance Parameter Setting block, (3) Harmonic Distortion Addition block, (4) AWGN addition block, and (5) MyDAQ data acquisition card. The first four blocks constitute the virtual instrument (VI) and are realized on LabVIEW software environment. VI-based design is divided in two segments: program code called block diagram and a GUI called front panel, both are powerfully integrated and linked with each other. The program code is implemented in LabVIEW block diagram for signal generation utilizing mathematical model of standard PQ disturbances suggested by IEEE Std.1159. A user-friendly and interactive GUI is designed on front panel for general parameter setting and amalgamation of real electrical conditions. The personal computer (PC) with LabVIEW is interfaced with MyDAQ via universal serial interface (USB). The instructions for generating the desired PQD signal with required disturbance parameters, level of noise, percentage of THD, and sampling rate are fetched through front panel. The designed program code in control panel scans the given commands and synthesizes the simulated PQD signal. The simulated PQD signal is converted into real-time voltage signal by MyDAQ, which can be obtained as output on its analog output channel specified in its general parameter setting. The presented PQD generator provides a comprehensive solution for the generation of specific single or multi-complex PQ signals with its defined parameters, including options to insert noise and harmonic distortion of specific levels. In general, proposed output on its analog output channel specified in its general parameter setting.

The presented PQD generator provides a comprehensive solution for the generation of specific single or multi-complex PQ signals with its defined parameters, including options to insert

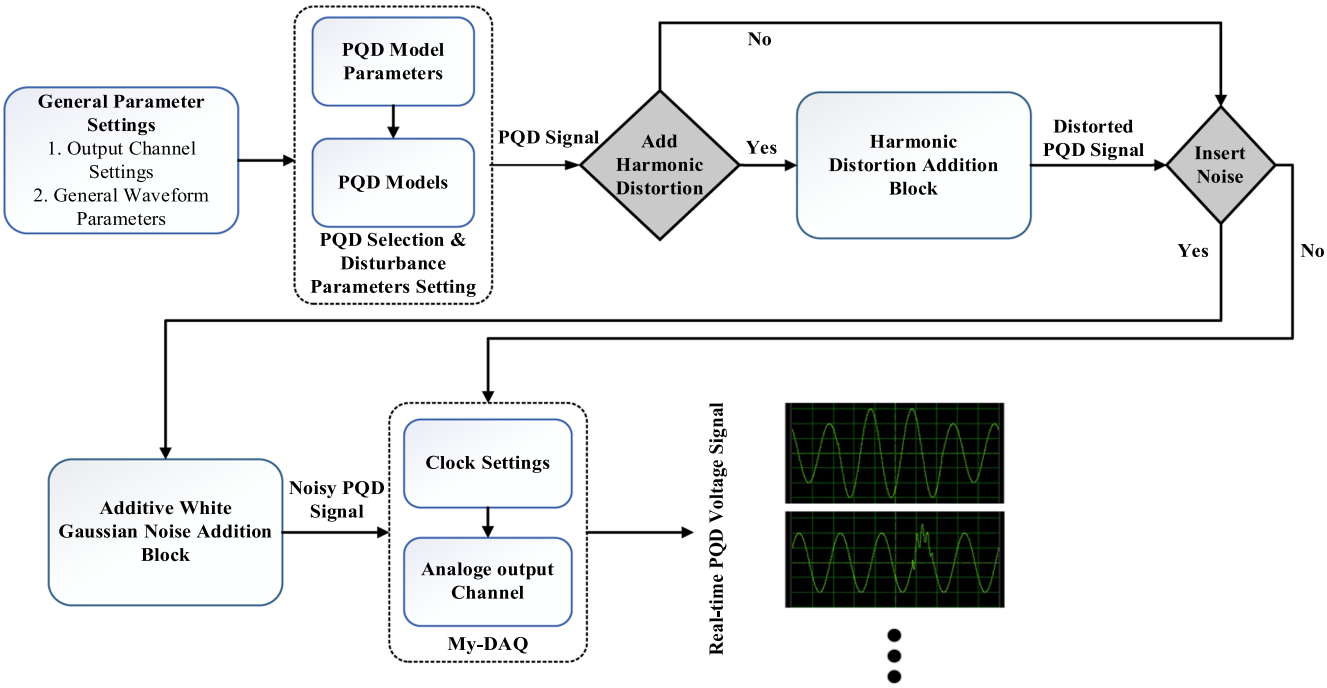

FIGURE 1 | Block diagram of proposed PQD generator.

20500505, 2026, 10, Downloaded from https://scijournals.onlinelibrary.wiley.com/doi/10.1002/ese3.70602 by Sheffield Hallam University, Wiley Online Library on [14/10/2026]. See the Terms and Conditions (https://onlinelibrary.wiley.com/terms-and-conditions) on Wiley Online Library for rules of use; OA articles are governed by the applicable Creative Commons License

noise and harmonic distortion of specific levels. In general, proposed instrument enables generation of three-phase signals. In current situation, it is developed for single-phase voltage waveform generation, but this scheme can be easily replicated in identical fashion in order to emulate a three-phase system. The forthcoming subsections provide a detailed explanation of the design and operations performed by each block of the PQD generator.

2.2 | General Parameter Settings Block

This block offers various choices for the selection of general parameters associated with the output waveform. These parameters are necessary to generate any specific disturbance waveform. Figure 2 shows the control panel designed (using LabVIEW front panel software module) for the selection of general parameter settings. The proposed generator gives flexibility of utilizing any of the data acquisition card provided by NI. The output channel of a particular NI data acquisition card can be chosen through the dropdown menu of "waveform setting" tab in the front panel. The output channel amplitude range and the generation mode, that is, continuous waveform or fixed waveform can also be selected using this VI. Selection of sampling frequency is crucial for the generation of a PQD voltage waveform. Sampling frequency is defined as the number of samples generated per second. Sampling rate should be selected according to the defined electrical power frequency. Because the wrong selection of sampling rate can produce an aliasing problem if the Nyquist criteria are violated. According to the Nyquist criteria, sampling frequency should be greater than twice the maximum frequency in the signal. The Fourier analysis of the PQD waveform synthesized using PQ standard models gives a maximum frequency component of 1.1 kHz. Therefore, sampling frequency must be greater than 2.2 kHz following the Nyquist criteria. The control panel provides flexibility of choosing the number of cycles to be generated that will define the duration of PQD waveform. This block is also responsible for setting the amplitude and power frequency of the sinusoidal waveform. A PQ disturbance detection and classification algorithm is necessarily implemented on an embedded controller for its application in real-time power quality monitoring. Most of the microcontrollers and other embedded controllers take positive voltage on their analog input channels. Considering the possibility of deploying PQ classification algorithm on such microcontrollers, the proposed PQD generator provides an option of adding the required DC offset in the sinusoidal waveform.

2.3 | PQD Selection and Disturbance Parameters Setting Block

One of the distinguished features of the proposed generator is its capability of generating the disturbance signal using the PQ mathematical equations provided by relevant IEEE standards. The disturbance waveforms are simulated through program code in the LabVIEW block diagram using PQ mathematical models. These models include various parameters associated with the characteristics of disturbance events. The PQD

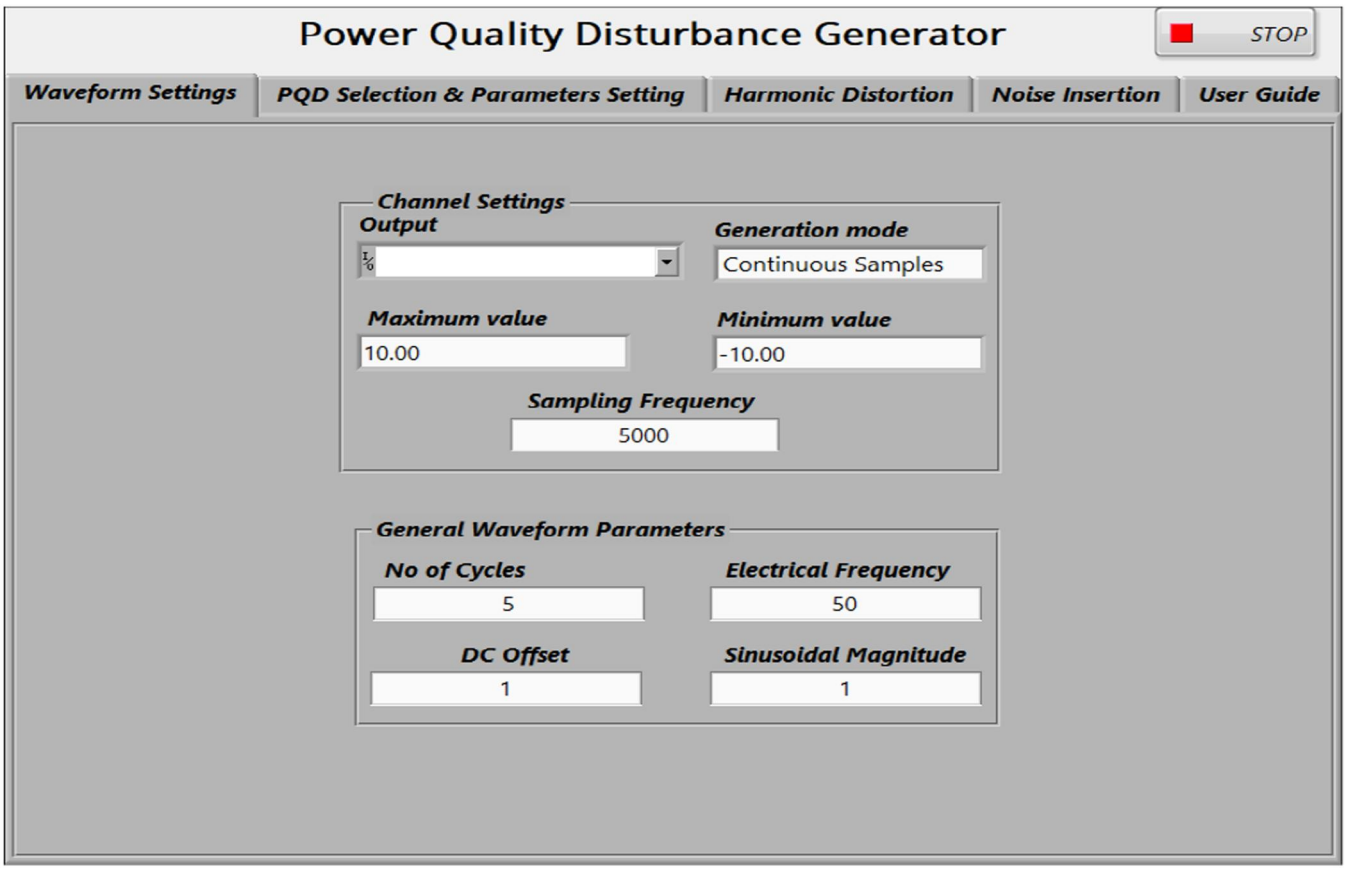

FIGURE 2 | Control panel for general parameter settings.

20500505, 2026, 10, Downloaded from https://scijournals.onlinelibrary.wiley.com/doi/10.1002/ese3.70602 by Sheffield Hallam University, Wiley Online Library on [14/10/2026]. See the Terms and Conditions (https://onlinelibrary.wiley.com/terms-and-conditions) on Wiley Online Library for rules of use; OA articles are governed by the applicable Creative Commons License

Selection and Disturbance Parameters Setting block provides options for the generation of 16 different types of PQD events according to the user-defined parameters. Most prominent parameters are listed as: disturbance duration (defined by start and end times), disturbance magnitude (for sag/swell related events), oscillatory transient-related parameters like phase, frequency, and time duration of one transient event, etc., harmonics-related parameters, flicker Frequency, and notch number (Figure 3).

Figure shows the GUI designed for the control of these parameters. Any event of desired characteristics can be generated using the above-mentioned models' parameters. Models also establish the bounds for each parameter, whether they are general or specific to disturbances. The description of 16 PQ models along with these mentioned parameters is given as follows:

2.4 | Normal or Pure Sinusoid

An ideal alternating voltage defined by sine trigonometric function having an exact RMS value of 707 mV is called Normal Sinusoid. It is defined by the following model.

$$v(t) = A\sin(\omega t - \varphi) \quad (1)$$

where $\omega = 2\pi f$ is the angular frequency in radian/sec.

φ = Phase angle in radians

A = Amplitude in Peak Unit

2.5 | Voltage Sag

Instantaneous decrease in the RMS amplitude of an alternating voltage is known as a voltage sag. Mathematically, it can be expressed as:

$$v_{sag}(t) = A(1 - \alpha(u(t - t_1) - u(t - t_2)))\sin(\omega t - \varphi) \quad (2)$$

where α = magnitude of voltage sag must be in the range (0.1, 0.9)

t_1 = Start time of voltage sag

t_2 = End time of Sag

Duration of voltage sag defined by t_1 and t_2 and must be in the range (T, $[N\text{-}1]\ T$) where T is the period of one cycle of sinusoid and N is the number of cycles.

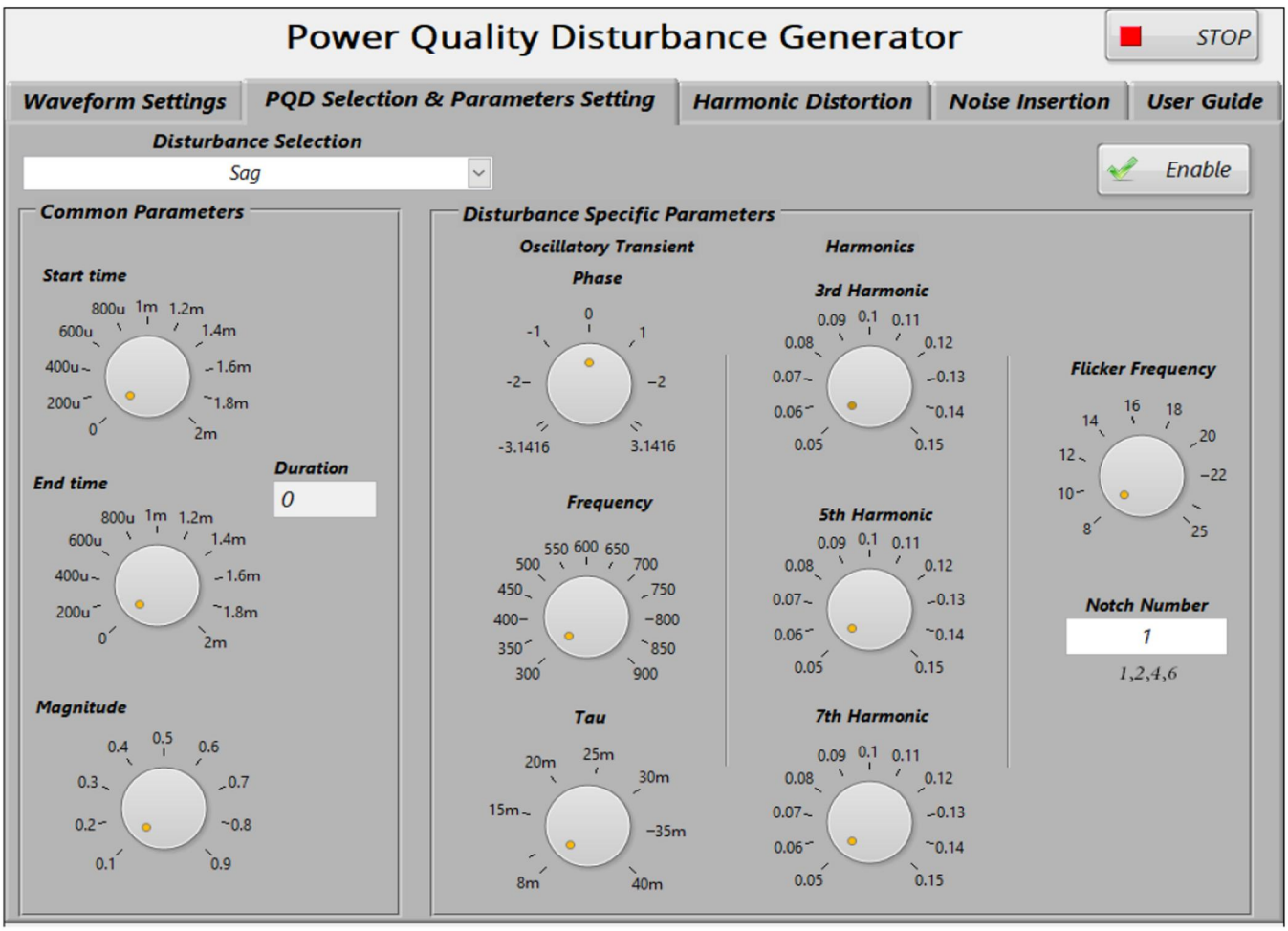

FIGURE 3 | Control panel for selection of different types of events and for setting of PQD model parameters.

20500505, 2026, 10, Downloaded from https://scijournals.onlinelibrary.wiley.com/doi/10.1002/ese3.70602 by Sheffield Hallam University, Wiley Online Library on [14/10/2026]. See the Terms and Conditions (https://onlinelibrary.wiley.com/terms-and-conditions) on Wiley Online Library for rules of use; OA articles are governed by the applicable Creative Commons License

2.6 | Voltage Swell

Voltage swell is an instantaneous increase in the RMS amplitude of sinusoid, mostly induced by energy storage elements at the time energy dissipation. Mathematical equation of swell is given as:

$$v_{swell}(t) = A(1 + \beta(u(t - t_1) - u(t - t_2)))\sin(\omega t - \varphi) \quad (3)$$

where β is the magnitude of Voltage Swell must be in the range (0.1, 0.8). Starting and end time of voltage swell are defined by t_1 and t_2, respectively. Duration of voltage is well defined by t_1 and t_2 and must be in the interval (*0, [N-1] T*).

2.7 | Voltage Interruption

Interruption is a special case of voltage sag. If the magnitude of voltage sag becomes greater than 90% of the nominal amplitude, then this condition is referred to as voltage interruption. Mathematical expression of interruption is given as:

$$v_{interruption}(t) = A(1 - \rho(u(t - t_1) - u(t - t_2))) \sin(\omega t - \varphi) \quad (4)$$

where ρ is the magnitude of interruption in the range (0.91, 1). t_1 and t_2 represent the start time and end time of the interruption event, respectively.

2.8 | Transient/Spike

Sudden change in the steady state of the nominal sinusoid is referred to as voltage transients/spikes. Mathematically, voltage transients can be expressed using the following equation.

$$v_{transient}(t) = A[\sin(\omega t - \varphi) - \psi(e^{-750(t-t_a)} - e^{-344(t-t_a)})(u(t - t_a) - u(t - t_b))] \quad (5)$$

where ψ is the magnitude of voltage transient. Duration of Voltage transient cannot be greater than 1 ms as referred from IEEE standard 1151. Start time and End time are defined by t_a and t_b=$t_a + 1$ ms, respectively, in the equation.

2.9 | Oscillatory Transient

Response of an electrical or electronic circuit toward voltage transient is known as oscillatory transient. Such voltage oscillations can only last for one and half cycles but can cause severe damage to the utility. It can be mathematically expressed as:

$$v_{O.T.}(t) = A[\sin(\omega t - \varphi) + \beta e^{-\frac{(t-t_I)}{\tau}}\sin(\omega_n(t - t_I) - \vartheta)(u(t - t_{II}) - u(t - t_I))] \quad (6)$$

where ω_n is the frequency of oscillation in (rad/s) in the range (600π, 1100π), ϑ is the phase angle of oscillations, and τ denotes the time duration of single transient in oscillations. Duration of oscillatory transient, defined by start time (t_I) and End time (t_{II}), must be in the range (0.05 T, NT/3.33).

2.10 | Flicker

Voltage flickering is a periodic but constant decrease in RMS amplitude of nominal sinusoid within specified frequency range. Mathematical model of flicker is given as:

$$v_{flicker}(t) = A[1 + \lambda\sin(\omega_f t)]\sin(\omega t - \varphi) \quad (7)$$

where λ denotes magnitude of flicker, must be in range (0.05, 0.1) and ω_f represents the frequency of flicker in rad/s, should be in the range (16π, 50π)

2.11 | Harmonics

Voltage harmonics are known as the addition of even or odd multiples of fundamental frequency in the nominal sinusoid. According to IEEE standard 1151, the allowed harmonic distortion in the voltage from the utility must be less than 5%. Mathematically harmonics can be expressed as:

$$v_{harmonic}(t) = \mathrm{A}\left[\sin(\omega t - \varphi) + \sum_{n=3}^{7}\alpha_n\sin(n\omega t - \vartheta_n)\right] \quad (8)$$

where α_n is the magnitude of nth harmonic ranging from 0.05 to 0.15, $n\omega$ is the nth multiple of fundamental sinusoidal frequency (rad/s), and ϑ_n is the phase angle in nth harmonic voltages.

2.12 | Notch

Periodic voltage spikes in the nominal sinusoid are known as notch. It lasts for duration less than 1 ms but can occur multiple times with periodicity. Each notch can occur maximum six times in one cycle as described by following mathematical expression.

$$v_{notch}(t) = A\left[\sin(\omega t - \varphi) - sign\left(\sin(\omega t - \varphi)\right) \sum_{n=0}^{N.c-1} k(u(t - (t_c + sn)) - u(t - (t_d + sn)))\right)\right] \quad (9)$$

where k = Magnitude of notch ranging from 0.1 to 0.4.

c = Number of Notch in each cycle.

s = Constraint of the end time of notch, $td \leq s$.

N = Number of cycles of nominal sinusoid.

Duration of Notch is defined by start time t_c and end time t_d and must be in the range (0.01 T, 0.05 T).

2.13 | Multi-Complex PQD Events

The combination of single disturbance events are known as multi-complex PQD events. Examples are sag with harmonics, flicker with sag, etc. Six different types of multi-complex events

20500505, 2026, 10, Downloaded from https://scijournals.onlinelibrary.wiley.com/doi/10.1002/ese3.70602 by Sheffield Hallam University, Wiley Online Library on [14/10/2026]. See the Terms and Conditions (https://onlinelibrary.wiley.com/terms-and-conditions) on Wiley Online Library for rules of use; OA articles are governed by the applicable Creative Commons License

are implemented in this study. They are listed as: flicker with sag, flicker with swell, sag with harmonics, swell with harmonics, sag with oscillatory Transient, and swell with oscillatory transient. Table 1 presents mathematical models of each complex PQD event with associated parameters.

2.14 | Noise Addition Block

In real-world electrical environment, noise is superimposed over voltage signals. Various sources, such as power electronic drives, control circuits, arcing devices, and loads with solid-state rectifiers, contribute to noise in the electric power system. This noise has the potential to degrade the performance of PQD detection and classification algorithms. This necessitates training and testing the algorithm on PQD signals, which are polluted with noise. Considering the requirement, proposed PQD generator has a special function that induces noise to the ideal disturbance voltage signal through its noise addition block. The noise level of real PQD waveforms in an electrical system is approximately 45 dB [37, 38]. However, the researchers need to validate the resilience of their proposed detection algorithm under more tough noisy conditions. For that purpose, the proposed generator is equipped with an option of adding/inserting additive white Gaussian noise (AWGN) of user's choice to ideal PQD signal with a signal-to-noise ratio (SNR) ranging from 30 to 80 dB. This gives an insight into the ability of a PQD monitoring system designed by researchers for working satisfactorily if implemented on a real system. Figure 4 shows the respective GUI for the generation of noisy PQD events generation.

2.15 | Harmonic Distortion Addition

The growing presence of harmonic sources such as wind parks, solar farms, HVDC stations, and static VAR compensators has highlighted the critical importance of voltage harmonics in both distribution and transmission systems [39]. Similarly, a range experimental assessments and modeling of harmonic distortion for energy efficient lighting and induction furnaces have been done in [40, 41]. To assess the influence of harmonic distortion on the efficacy of a PQD monitoring system, it is essential to train and test a detection algorithm using distorted PQD signals. The Harmonic Distortion Addition block of the designed PQD generator provides features of adding harmonic distortion to the ideal PQD signal. Although IEEE std. 519 permits 5% voltage distortion in a distribution network, however proposed PQD generator has the option of inducing harmonic distortion up to any user-defined level up to 13th component (Odd only). Figure 5 depicts the respective panel of the VI for incorporating harmonic distortion into the PQD event.

TABLE 1 | Mathematical models of multi-complex power quality disturbance events.

PQD event	Name	Mathematical model	Constraints
10	Flicker with Sag	$A[1+\lambda\sin(\omega_f t)]\sin(\omega t-\varphi)+$ $A(1-\alpha(u(t-t_1)-u(t-t_2)))\sin(\omega t-\varphi)$	$0.05\le\lambda\le0.1$ $8\le f_f\le25Hz,\ \omega_f=2\pi f_f$ $T\le t_2-t_1\le(N-1)T$ $0.1\le\alpha\le0.9$
11	Flicker with Swell	$A[1+\lambda\sin(\omega_f t)]\sin(\omega t-\varphi)+$ $A(1+\beta(u(t-t_1)-u(t-t_2)))\sin(\omega t-\varphi)$	$0.05\le\lambda\le0.1$ $8\le f_f\le25Hz,\ \omega_f=2\pi f_f$ $T\le t_2-t_1\le(N-1)T$ $0.1\le\beta\le0.9$
12	Sag with Harmonics	$A(1-\alpha(u(t-t_1)-u(t-t_2)))\sin(\omega t-\varphi)$ $+\mathrm{A}[\sin(\omega t-\varphi)+\sum_{n=3}^{7}\alpha_n\sin(n\omega t-\vartheta_n)]$	$T\le t_2-t_1\le(N-1)T$ $0.1\le\alpha\le0.9$ $n=\{3,5,7\};\ 0.05\le\alpha_n\le0.15$ $-\pi\le\vartheta_n\le\pi$
13	Swell with Harmonics	$A(1+\beta(u(t-t_1)-u(t-t_2)))\sin(\omega t-\varphi)$ $+\mathrm{A}[\sin(\omega t-\varphi)+\sum_{n=3}^{7}\alpha_n\sin(n\omega t-\vartheta_n)]$	$T\le t_2-t_1\le(N-1)T$ $0.1\le\beta\le0.9$ $n=\{3,5,7\};\ 0.05\le\alpha_n\le0.15$ $-\pi\le\vartheta_n\le\pi$
14	Sag with Oscillatory Transient	$A(1-\alpha(u(t-t_1)-u(t-t_2)))\sin(\omega t-\varphi)$ $+A[\sin(\omega t-\varphi)+\beta e^{-\frac{(t-t_I)}{\tau}}\sin(\omega_n(t-t_I)-\vartheta)$ $(u(t-t_{II})-u(t-t_I))]$	$T\le t_2-t_1\le(N-1)T$ $0.1\le\alpha\le0.9$ $300\le f_n\le900Hz$ $\omega_n=2\pi f_n;8ms\le\tau\le40ms$ $-\pi\le\vartheta\le\pi$ $0.05T\le t_{II}-t_I\le\frac{N}{3.33}T$
15	Swell with Oscillatory Transient	$A(1+\beta(u(t-t_1)-u(t-t_2)))\sin(\omega t-\varphi)$ $+A[\sin(\omega t-\varphi)+\beta e^{-\frac{(t-t_I)}{\tau}}\sin(\omega_n(t-t_I)-\vartheta)$ $(u(t-t_{II})-u(t-t_I))]$	$\le t_2-t_1\le(N-1)T$ $0.1\le\beta\le0.9$ $300\le f_n\le900Hz$ $\omega_n=2\pi f_n;8ms\le\tau\le40ms$ $-\pi\le\vartheta\le\pi$ $0.05T\le t_{II}-t_I\le\frac{N}{3.33}T$

20500505, 2026, 10, Downloaded from https://scijournals.onlinelibrary.wiley.com/doi/10.1002/ese3.70602 by Sheffield Hallam University, Wiley Online Library on [14/10/2026]. See the Terms and Conditions (https://onlinelibrary.wiley.com/terms-and-conditions) on Wiley Online Library for rules of use; OA articles are governed by the applicable Creative Commons License

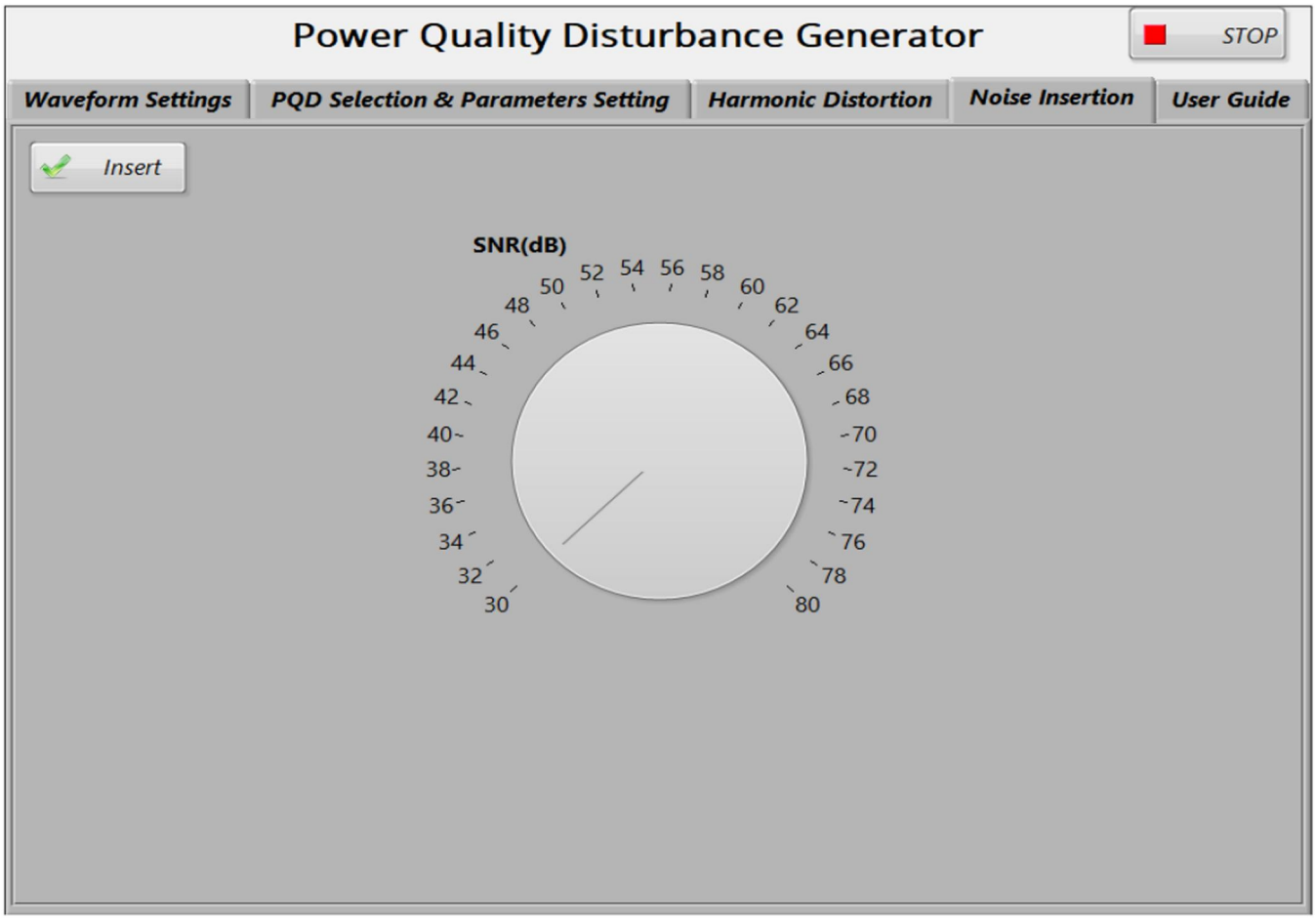

FIGURE 4 | Control panel for insertion of AWGN noise.

2.16 | Generation of Real-Time PQD Events Using MyDAQ

The resultant PQD signal, either with or without noise and harmonic distortion, is written to the data acquisition card for real-time generation. MyDAQ provided by the National Instruments (NI) is used for this purpose. The General Settings Panel of the VI allows direct control over MyDAQ operations, such as finite and continuous samples generation, sampling rate, channel amplitude constraint, and the number of samples to be produced at the output in a single cycle. This control is facilitated by parameter settings such as power frequency, number of cycles, DC bias, and sampling rate. Figure 6 illustrates the program code (block diagram) of the VI developed in the LabVIEW programming environment.

3 | Experimental Setup for Verification of PQD Generator

Figure 7 shows the experimental setup for the analysis and verification of waveforms generated by proposed PQD generator. The generated PQD signal is obtained at the analog output channel of MyDAQ. The output of PQD generator is connected to the oscilloscope of NI ELVIS II from NI through input channel. NI ELVIS II is connected to a personal computer via USB. All the waveforms and associated results were observed on computer-based oscilloscope using NI Instrument Launcher software application. Different PQD events were generated using proposed PQD generator and visualized through oscilloscope. Some typical/exemplary PQD waveforms were generated and logged in computer using settings shown in Table 2. Figures 8–14 shows the signals generated by the proposed PQD generator.

4 | Measurement Uncertainty Results

The reliability of an instrument is a critical consideration for both commercial and laboratory applications. Measuring the results produced by an instrument determines its reliability and conformity. The quality of results significantly influences the decision about deployment of instruments in a particular application based on measurements. Calculating the measurement uncertainty of an instrument provides an insight about the quality of results [42]. The measurement uncertainty is computed according to the steps outlined by the Guide to the Expression of Uncertainty in Measurement [43], by the International Organization for Standardization. The measurement uncertainty of the proposed PQD generator includes the determination of voltage uncertainty and frequency uncertainty, detailed in the subsequent subsections.

4.1 | Voltage Uncertainty

The uncertainty of the RMS voltage was calculated using measurements obtained from waveforms generated by the

20500505, 2026, 10, Downloaded from https://scijournals.onlinelibrary.wiley.com/doi/10.1002/ese3.70602 by Sheffield Hallam University, Wiley Online Library on [14/10/2026]. See the Terms and Conditions (https://onlinelibrary.wiley.com/terms-and-conditions) on Wiley Online Library for rules of use; OA articles are governed by the applicable Creative Commons License

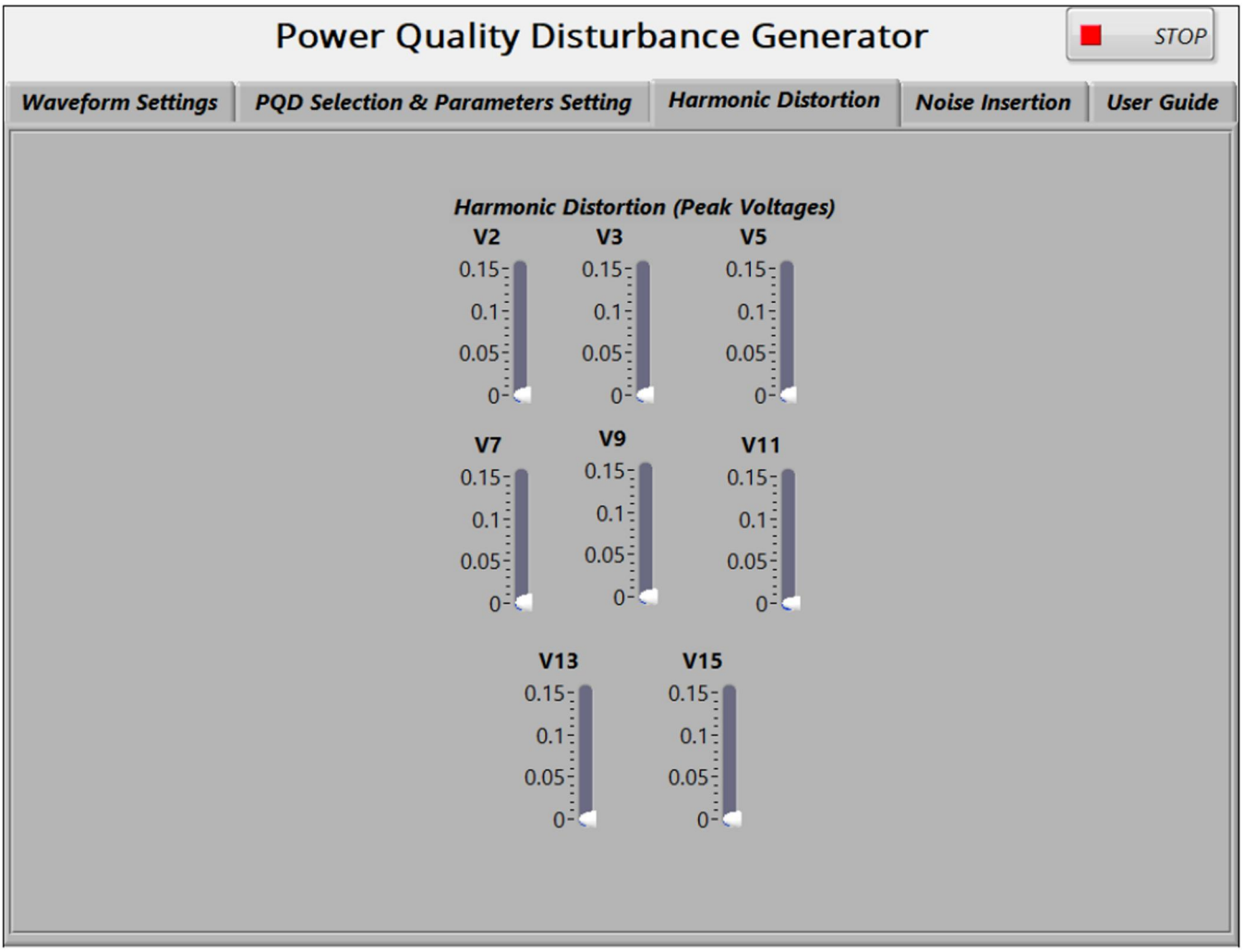

FIGURE 5 | Control panel for adding harmonic distortion.

proposed PQD generator. Waveforms with a nominal RMS voltage of 5 V were generated by the proposed instrument and measured using an oscilloscope. Measurements were taken both without harmonic distortion and with THD of 5%, 10%, and 15% at two different signal frequencies, 50 and 60 Hz. To calculate uncertainty, a total of 10 measurements were taken at each signal frequency, both with and without harmonic distortion. Table 3 presents the recorded measurements at two nominal voltages of 5 and 7.07 V without harmonic distortion at signal frequencies of 50 Hz, 1 kHz, and 2.5 kHz. The uncertainty of the RMS voltage is computed using the relation described in Equation 10.

$$V_Uncertainty = \sqrt{\frac{1}{n(n-1)}\sum_{i=1}^{n}(V_{rms} - V_{average})^2} \quad (10)$$

Table 3 reveals that the minimum uncertainty of 6.102 μV occurs with a nominal voltage of 7.07 V at a signal frequency of 50 Hz, while the maximum uncertainty of 32.28 μV is observed at a signal frequency of 1 kHz. Additionally, it is evident that at a higher voltage of 7.07 V, the uncertainty is notably larger than that at 5 V, confirming a direct relationship between uncertainty and nominal RMS voltage. An increasing trend in voltage uncertainty is also observed with an increase in signal frequency. However, overall voltage uncertainties of the proposed PQD generator at different frequencies remain very small.

Tables 4–6 illustrate the impact of harmonic distortion on the voltage uncertainty of the generator. Table 4 presents voltage measurements recorded at 5% harmonic distortion along with uncertainty calculations. The addition of harmonic distortion does not significantly affect voltage uncertainty at the nominal frequency of 50 Hz. At higher frequencies, a minor change is observed in voltage uncertainty, increasing from 14.4 to 264 μV due to the addition of harmonic distortion, considering the case for a nominal voltage of 5 V with a signal frequency of 1 kHz. Similarly, at a frequency of 2.5 kHz, uncertainty increases from 20.5 to 538 μV. Compared to ideal signals, the addition of harmonic distortion affects measurement uncertainty; however, these results demonstrate that uncertainty values are still acceptably small. Tables 5 and 6 show recorded measurements at 10% and 15% harmonic distortions with computed measurement uncertainty results. No significant change is observed in voltage uncertainty at higher harmonic distortion. The results obtained at different nominal voltages, harmonic distortions, and signal frequencies indicate that the change in measurement uncertainty is not very significant, highlighting

20500505, 2026, 10, Downloaded from https://scijournals.onlinelibrary.wiley.com/doi/10.1002/ese3.70602 by Sheffield Hallam University, Wiley Online Library on [14/10/2026]. See the Terms and Conditions (https://onlinelibrary.wiley.com/terms-and-conditions) on Wiley Online Library for rules of use; OA articles are governed by the applicable Creative Commons License

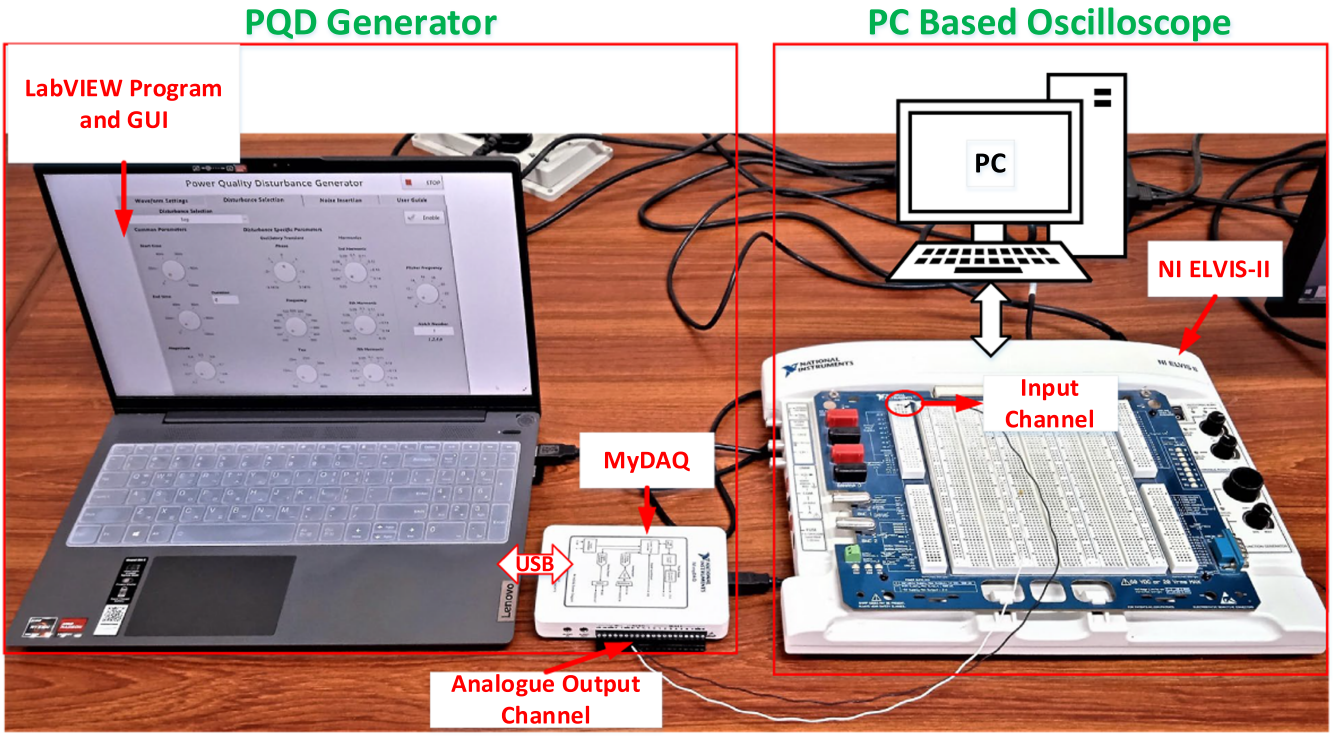

FIGURE 6 | Block diagram of power quality disturbance generator developed in LabVIEW programing environment.

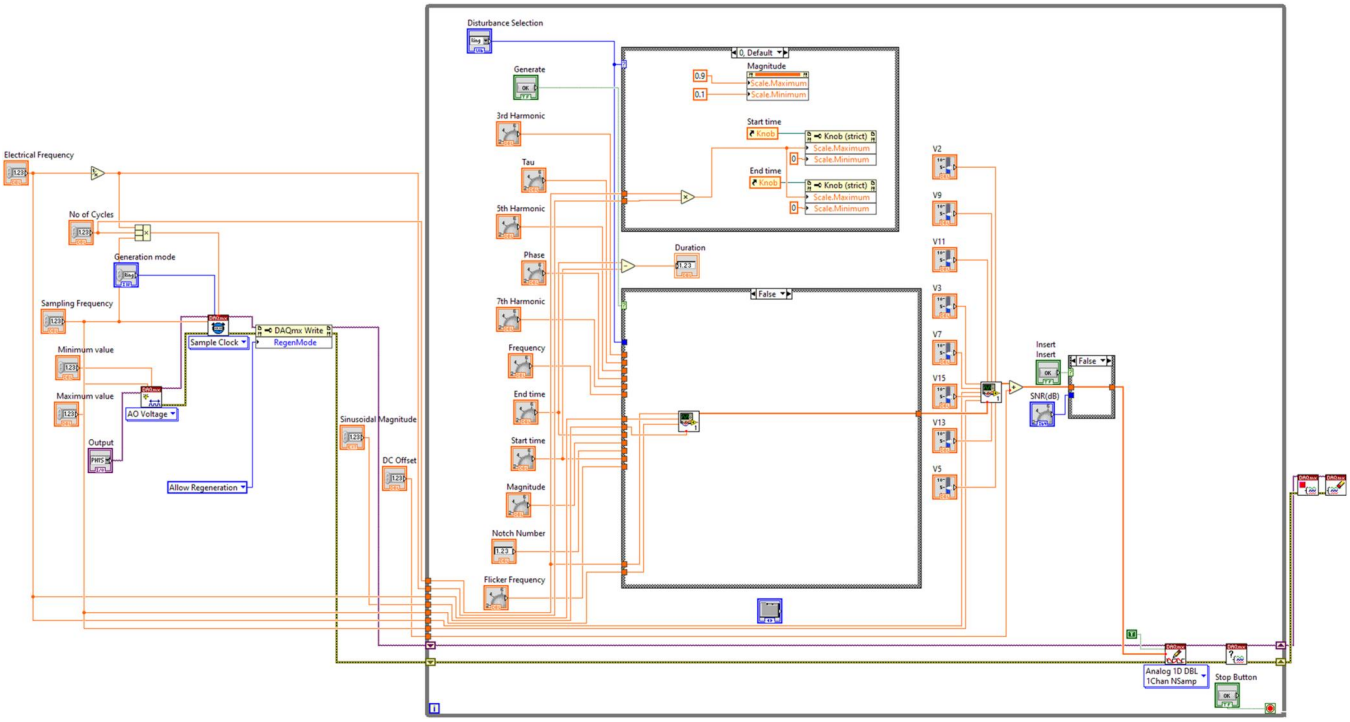

FIGURE 7 | Experimental setup for verification of proposed PQD generator.

TABLE 2 | Typical PQD waveforms setting.

Sampling frequency	5 kHz
Number of cycles per trigger	5
Sinusoidal amplitude	1 V_p (or 707 mV in RMS units)
Electrical frequency	50 Hz

the reliability and conformity of the proposed PQD generator for use in various relevant applications.

Quantitatively, the effect of harmonic distortion on voltage uncertainty is frequency-dependent. At the nominal frequency of 50 Hz, the uncertainty remains in the microvolt range. For the 5 V RMS case, the uncertainty changes from 10.21 μV without harmonic distortion to 6.19–14.54 μV under 5%–15% harmonic distortion.

20500505, 2026, 10, Downloaded from https://scijournals.onlinelibrary.wiley.com/doi/10.1002/ese3.70602 by Sheffield Hallam University, Wiley Online Library on [14/10/2026]. See the Terms and Conditions (https://onlinelibrary.wiley.com/terms-and-conditions) on Wiley Online Library for rules of use; OA articles are governed by the applicable Creative Commons License

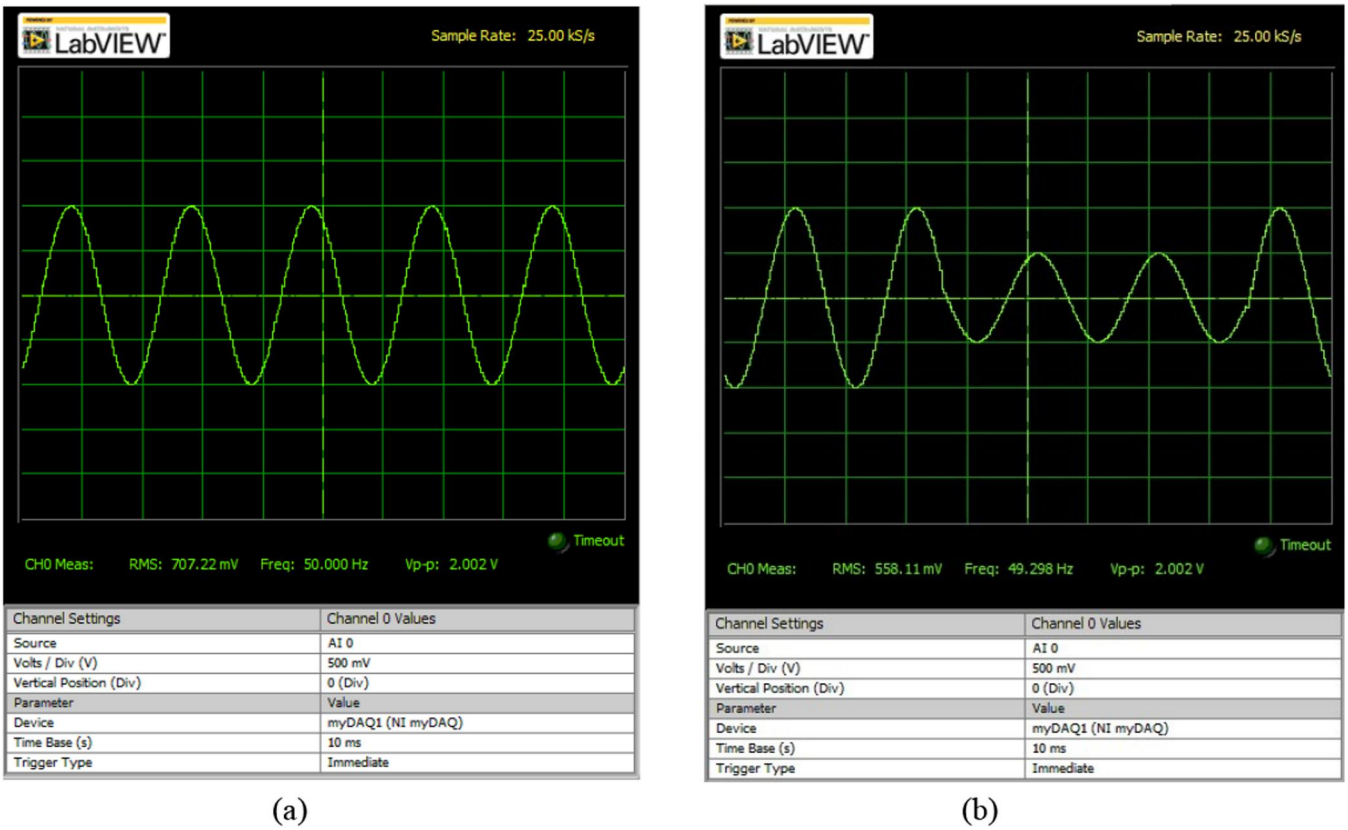

FIGURE 8 | Real-time signals visualized using NI ELVIS II: (a) Normal, (b) Sag.

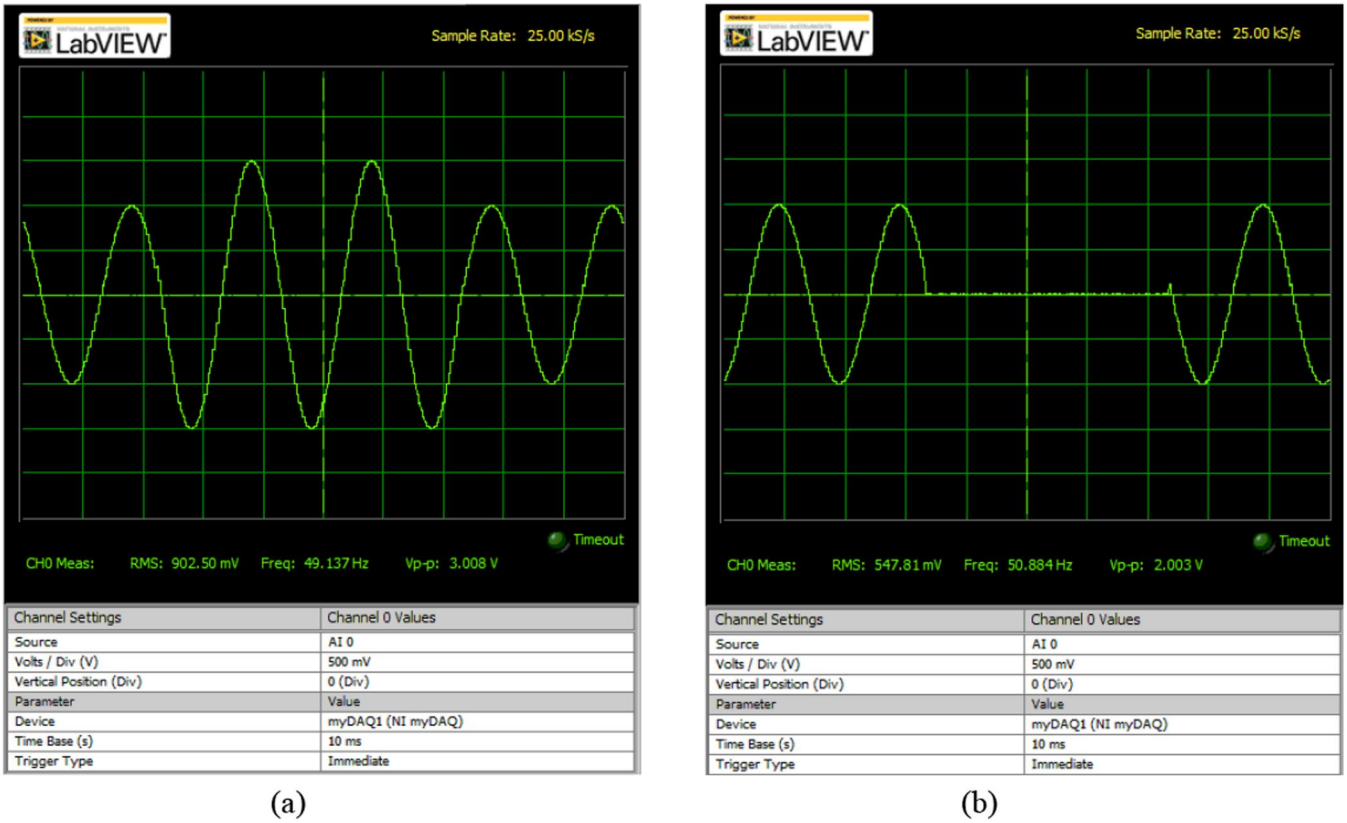

FIGURE 9 | Real-time signals visualized using NI ELVIS II: (a) Swell, (b) Interruption.

20500505, 2026, 10, Downloaded from https://scijournals.onlinelibrary.wiley.com/doi/10.1002/ese3.70602 by Sheffield Hallam University, Wiley Online Library on [14/10/2026]. See the Terms and Conditions (https://onlinelibrary.wiley.com/terms-and-conditions) on Wiley Online Library for rules of use; OA articles are governed by the applicable Creative Commons License

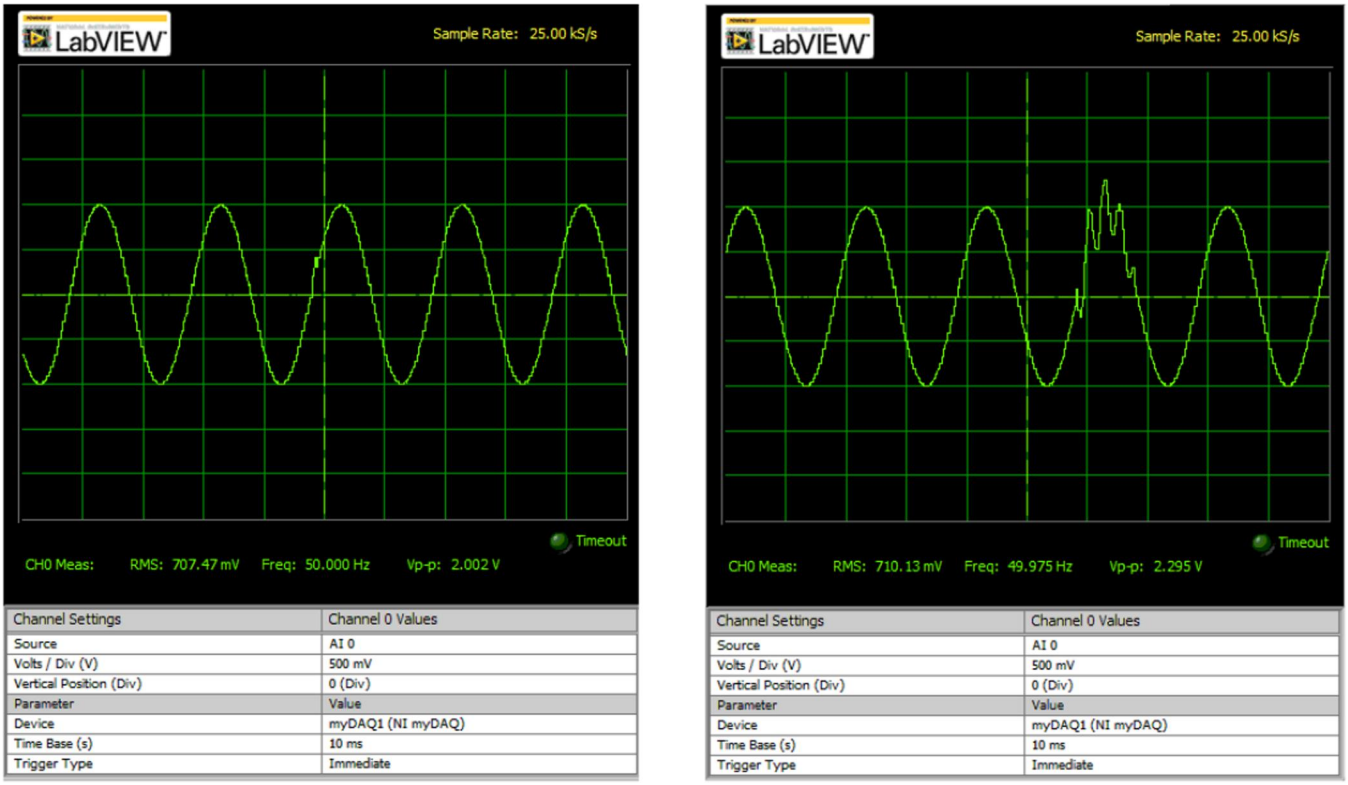

FIGURE 10 | Real-time signals visualized using NI ELVIS II: (a) Transient, (b) Oscillatory Transient.

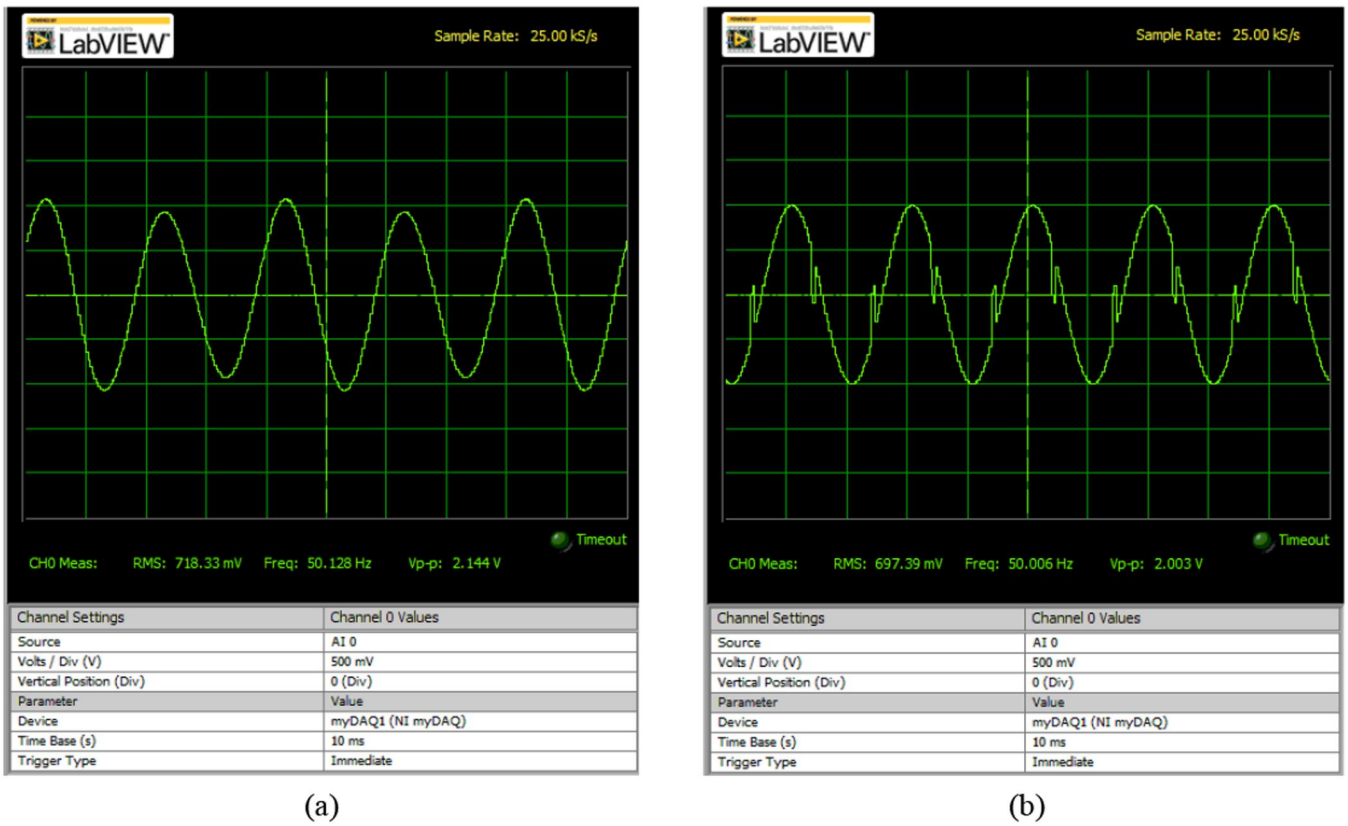

FIGURE 11 | Real-time signals visualized using NI ELVIS II: (a) Flicker, (b) Notch.

20500505, 2026, 10, Downloaded from https://scijournals.onlinelibrary.wiley.com/doi/10.1002/ese3.70602 by Sheffield Hallam University, Wiley Online Library on [14/10/2026]. See the Terms and Conditions (https://onlinelibrary.wiley.com/terms-and-conditions) on Wiley Online Library for rules of use; OA articles are governed by the applicable Creative Commons License

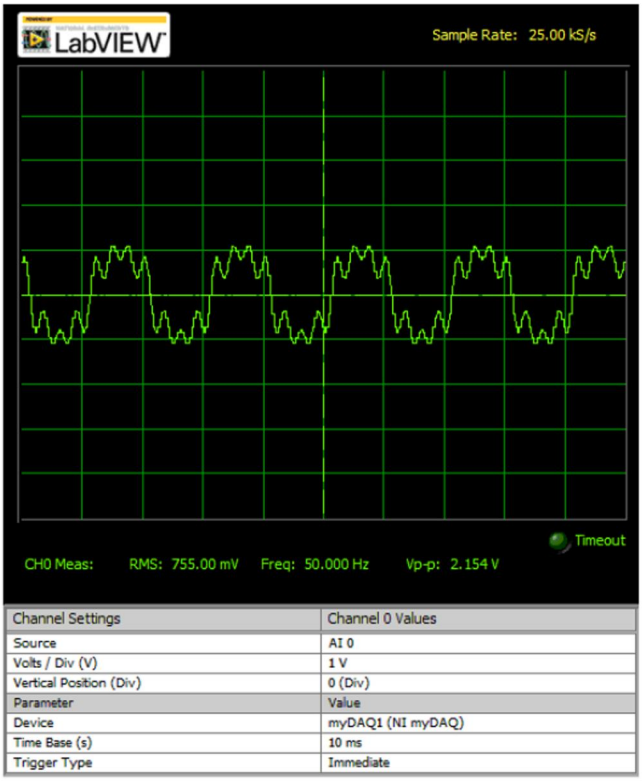

(a)

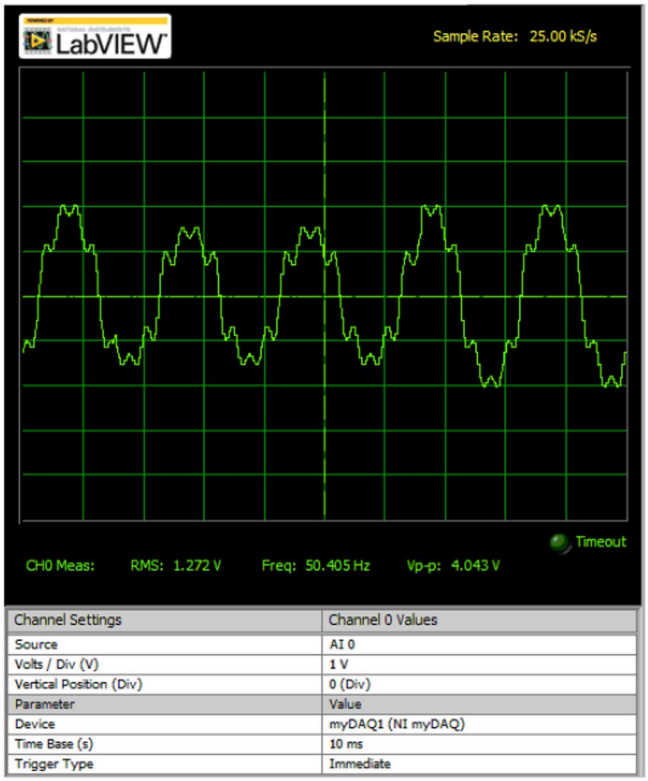

(b)

FIGURE 12 | Real-time signals visualized using NI ELVIS II: (a) Harmonics, (b) Harmonics with Sag.

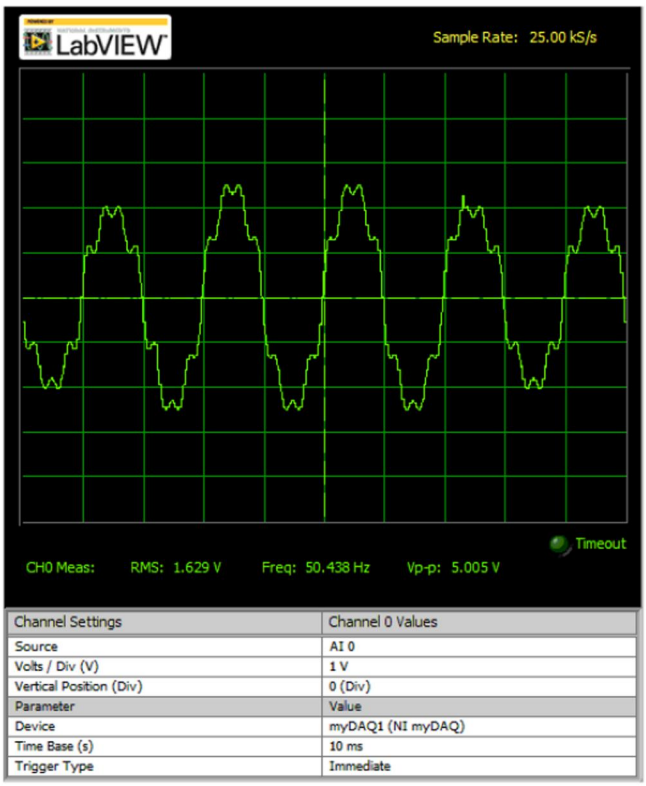

(a)

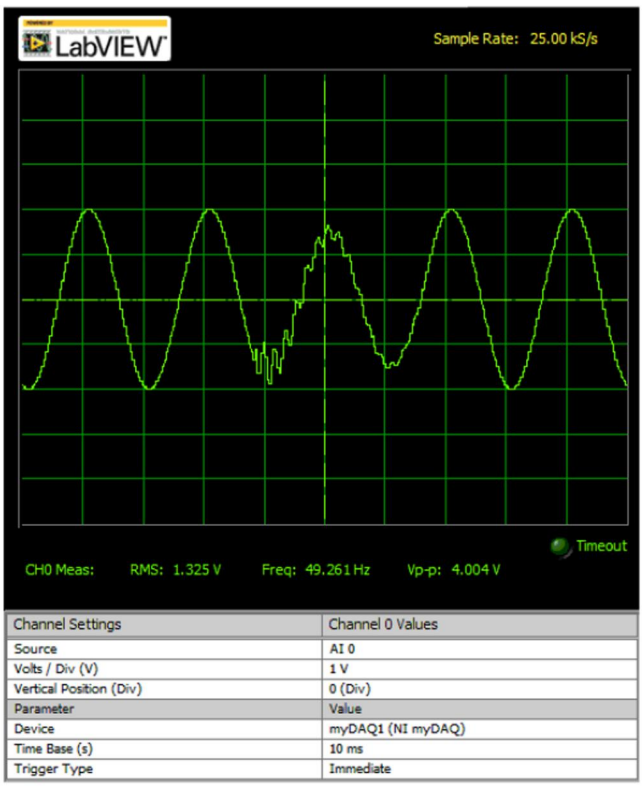

(b)

FIGURE 13 | Real-time signals visualized using NI ELVIS II: (a) Harmonics with Swell, (b) Sag with oscillatory transient.

20500505, 2026, 10, Downloaded from https://scijournals.onlinelibrary.wiley.com/doi/10.1002/ese3.70602 by Sheffield Hallam University, Wiley Online Library on [14/10/2026]. See the Terms and Conditions (https://onlinelibrary.wiley.com/terms-and-conditions) on Wiley Online Library for rules of use; OA articles are governed by the applicable Creative Commons License

(a) (b)

FIGURE 14 | Real-time signals visualized using NI ELVIS II: (a) Flicker with Sag, (b) Flicker with Swell.

For the 7.07 V RMS case, it changes from 6.29 μV to 12.99–35.92 μV. Therefore, harmonic distortion has only a small absolute impact on voltage uncertainty at 50 Hz. At higher frequencies, the increase is more visible. For 5 V RMS, the maximum uncertainty increases from 14.45 to 285 μV at 1 kHz and from 20.52 to 656 μV at 2.5 kHz. For 7.07 V RMS, the maximum uncertainty increases from 32.28 to 444 μV at 1 kHz and from 16.14 to 982 μV at 2.5 kHz. However, even in the worst case, the voltage uncertainty remains below 1 mV, corresponding to less than 0.014% of the nominal RMS voltage. These results show that harmonic distortion increases voltage uncertainty mainly at higher frequencies, but the absolute uncertainty remains sufficiently low for laboratory-level PQD generation.

4.2 | Frequency Uncertainty

To assess the frequency uncertainty of the PQD generator, signals with various frequencies were generated, and frequency measurements were recorded using the NI ELVIS II oscilloscope. Throughout these experiments, the RMS voltage was maintained at a constant 5 V. Ten measurements were recorded at each frequency, both with and without harmonic distortions. Uncertainty is calculated using the following equation.

$$f_Uncertainty = \sqrt{\frac{1}{n(n-1)}\sum_{i=1}^{n}(f_i - f_{average})^2} \tag{11}$$

Table 7 presents the computed values of standard deviation and uncertainty for frequencies of 50 Hz, 1 kHz, and 2.5 kHz without harmonic distortions. Frequency uncertainty of the PQD generator at 50 Hz frequency was found to be 0.3 μHz. This shows a tremendous sense of reliability of the proposed instrument. Similarly, very small uncertainty values of 85 μHz and 0.0003995 Hz were obtained at frequencies of 2.5 and 1 kHz, respectively, without harmonic distortion. Results obtained without harmonic distortion are somewhat approximated as ideal. A variation of frequency uncertainty was observed on the addition of harmonics to nominal sinusoid as depicted in Tables 8–10. Table 8 represents the calculated uncertainty in frequency with 5% harmonic distortion at different signal frequencies. A trivial change can be observed at higher frequencies compared to Table 1. Uncertainty of 9.3 mHz was obtained at a frequency of 2.5 kHz. Similarly, Tables 9 and 10 represent the calculated uncertainty in frequency with 10% and 15% harmonic distortions, respectively.

The quantitative effect of harmonic distortion on frequency uncertainty is also limited in absolute terms. Without harmonic distortion, the frequency uncertainty is 0.030 mHz at 50 Hz, 0.3995 mHz at 1 kHz, and 0.0859 mHz at 2.5 kHz. Under 5%–15% harmonic distortion, the uncertainty ranges from 0.0809 to 0.510 mHz at 50 Hz, from 5.9385 to 6.0505 mHz at 1 kHz, and from 0.1871 to 9.8867 mHz at 2.5 kHz. Although the relative increase appears large at higher frequencies because the baseline uncertainty is extremely small, the maximum observed frequency uncertainty remains below 10 mHz. This corresponds to less than 0.0011% of the nominal frequency across the tested cases. Hence, harmonic distortion produces a measurable but practically small increase in frequency uncertainty.

The proposed PQD Generator in this article demonstrates reliability in terms of performance and uncertainty when

20500505, 2026, 10, Downloaded from https://scijournals.onlinelibrary.wiley.com/doi/10.1002/ese3.70602 by Sheffield Hallam University, Wiley Online Library on [14/10/2026]. See the Terms and Conditions (https://onlinelibrary.wiley.com/terms-and-conditions) on Wiley Online Library for rules of use; OA articles are governed by the applicable Creative Commons License

TABLE 3 | Measurement results and uncertainty without harmonic distortion – PQD generator RMS voltages.

(For 50 Hz Frequency)						
Voltage (RMS)	**5 V**			**7.07 V**		
Frequency (Hz)	**50**	**1000**	**2500**	**50**	**1000**	**2500**
No of measurements						
1	5.005861	5.006061	5.005762	7.080264	7.080311	7.080519
2	5.005925	5.005994	5.005768	7.080222	7.080233	7.080432
3	5.005925	5.006003	5.005762	7.08025	7.08023	7.080418
4	5.005881	5.006058	5.00569	7.08028	7.079931	7.080388
5	5.005955	5.00605	5.005789	7.080235	7.08021	7.080501
6	5.005948	5.005916	5.005791	7.08022	7.080185	7.080539
7	5.00594	5.006032	5.005782	7.080268	7.080163	7.080436
8	5.005938	5.006036	5.005883	7.080235	7.080248	7.080474
9	5.005951	5.006034	5.005889	7.080255	7.08013	7.080487
10	5.005894	5.006072	5.005881	7.080242	7.080216	7.080525
Uncertainty calculation						
ST. DEV	3.06425E-05	4.33502E-05	6.15696E-05	1.8865E-05	9.68401E-05	4.84199E-05
ST. DEV/$\sqrt{n}$	9.68999E-06	1.37085E-05	1.947E-05	5.96565E-06	3.06235E-05	1.53117E-05
$V_{average}$ *(V)*	5.0059218	5.0060256	5.0057997	7.0802471	7.0801857	7.0804719
V_Uncertainty (V)	1.02142E-05	1.44501E-05	2.05232E-05	6.28835E-06	3.228E-05	1.614E-05

TABLE 4 | Measurement results and uncertainty with 5% harmonic distortion – PQD generator RMS voltages.

(For 50 Hz, 1 kHz, 2.5 kHz Frequency)						
Voltage (RMS)	**5 V**			**7.07 V**		
Frequency (Hz)	**50**	**1000**	**2500**	**50**	**1000**	**2500**
No of measurements						
1	5.006483	5.006427	5.005876	7.08078	7.080736	7.078985
2	5.006454	5.004412	5.004842	7.080771	7.077534	7.080546
3	5.006416	5.005886	5.006258	7.080833	7.078006	7.077588
4	5.006489	5.006423	5.005814	7.080806	7.08074	7.072545
5	5.006494	5.006435	5.00384	7.080766	7.080725	7.080586
6	5.006511	5.005428	5.006399	7.080913	7.080682	7.080494
7	5.006471	5.006068	5.000956	7.080814	7.077757	7.078392
8	5.006495	5.006323	5.006038	7.081049	7.080342	7.077986
9	5.006512	5.004816	5.006049	7.080741	7.080485	7.080541
10	5.006479	5.00443	5.006301	7.080809	7.080821	7.074708
Uncertainty computation						
ST. DEV	2.71079E-05	0.000791	0.001613	8.608E-05	0.001331	0.002592
ST. DEV/$\sqrt{n}$	8.57228E-06	0.00025	0.00051	2.72209E-05	0.000421	0.00082
$V_{average}$ *(V)*	5.0064804	5.005665	5.005237	7.0808282	7.079783	7.078237
V_Uncertainty (V)	9.03598E-06	0.000264	0.000538	2.86933E-05	0.000444	0.000864

compared to the generation methods discussed in the literature. It proves to be efficient for laboratory-level analysis and the generation of various PQD events for research purposes. The functionality of the proposed generator can be readily updated to generate 35 types of PQD events. Furthermore, the performance of the generator can be enhanced in terms of measurement uncertainty by utilizing a DAQ card with a higher sampling rate.

5 | Comparison of PQD Generator With Available Commercial PQ Signal Generation Instruments

The LabVIEW-based PQD generator was compared with commercially available instruments, to evaluate its technical performance. Table 11 illustrates the comparison between three instruments, including Keysight-6811B, Calmet C300, and Metrel M12191 [44–46]. The comparison reveals that the proposed

20500505, 2026, 10, Downloaded from https://scijournals.onlinelibrary.wiley.com/doi/10.1002/ese3.70602 by Sheffield Hallam University, Wiley Online Library on [14/10/2026]. See the Terms and Conditions (https://onlinelibrary.wiley.com/terms-and-conditions) on Wiley Online Library for rules of use; OA articles are governed by the applicable Creative Commons License

TABLE 5 | Measurement results and uncertainty with 10% harmonic distortion—PQD generator RMS voltages.

(For 50 Hz, 1 kHz, 2.5 kHz Frequency)						
Voltage (RMS)	**5 V**			**7.07 V**		
Frequency (Hz)	**50 Hz**	**1000**	**2500**	**50 Hz**	**1000**	**2500**
No of measurements						
1	5.006481	5.006345	5.003779	7.080708	7.078363	7.079586
2	5.006448	5.006342	5.005987	7.080716	7.079654	7.078764
3	5.006462	5.00413	5.004873	7.080748	7.077371	7.071804
4	5.006471	5.006314	5.003071	7.080695	7.077827	7.078569
5	5.00646	5.00527	5.004631	7.080996	7.077358	7.079278
6	5.006505	5.006102	5.002206	7.080958	7.077232	7.074441
7	5.006448	5.004277	5.005316	7.080745	7.078858	7.078448
8	5.006491	5.005943	5.005902	7.080708	7.079183	7.07109
9	5.006458	5.006277	5.006139	7.080702	7.077467	7.076013
10	5.00649	5.004684	5.006115	7.080681	7.077938	7.077249
Uncertainty computation						
ST. DEV	1.85591E-05	0.00085397	0.00131173	0.000107758	0.00081007	0.00294608
ST. DEV/$\sqrt{n}$	5.8689E-06	0.00027005	0.00041481	3.40761E-05	0.00025617	0.00093163
$V_{average}$ *(V)*	5.0064714	5.0055684	5.0048019	7.0807657	7.0781251	7.0765242
V_Uncertainty (V)	6.18636E-06	0.000285	0.000437	3.59194E-05	0.00027	0.000982

TABLE 6 | Measurement results and uncertainty with 15% harmonic distortion—PQD generator RMS voltages.

(For 50 Hz, 1 kHz, 2.5 kHz frequency)						
Voltage (RMS)	**5 V**			**7.07 V**		
Frequency (Hz)	**50 Hz**	**1000**	**2500**	**50 Hz**	**1000**	**2500**
No of measurements						
1	5.007355	5.006685	5.003693	7.081306	7.079848	7.072819
2	5.007378	5.007285	5.007047	7.08129	7.081014	7.080941
3	5.00734	5.007249	5.006885	7.081356	7.081063	7.078631
4	5.007494	5.007152	5.007056	7.081281	7.081037	7.080952
5	5.00737	5.006275	5.006403	7.081267	7.081074	7.080114
6	5.007375	5.007088	5.000574	7.081335	7.078879	7.080167
7	5.00736	5.0073	5.004562	7.081318	7.081006	7.080233
8	5.007383	5.007256	5.006339	7.081205	7.080843	7.080348
9	5.00733	5.007165	5.00674	7.081284	7.081085	7.080555
10	5.007408	5.006554	5.004709	7.081295	7.080495	7.080638
Uncertainty computation						
ST. DEV	4.36327E-05	0.0003436	0.00196793	3.89616E-05	0.00069189	0.00232478
ST. DEV/$\sqrt{n}$	1.37979E-05	0.00010866	0.00062231	1.23208E-05	0.00021879	0.00073516
$V_{average}$ *(V)*	5.0073793	5.0070009	5.0054008	7.0812937	7.0806344	7.0795398
V_Uncertainty (V)	1.45442E-05	0.000115	0.000656	1.29872E-05	0.000231	0.000775

PQD generator outperforms commercially available instruments in terms of measurement uncertainty, exhibiting the lowest uncertainty in both voltage and frequency. This highlights the reliability level of the instrument. Like high-cost commercial instruments, the proposed PQD generator implements PQ disturbance models provided by relevant standards and includes short-circuit protection. Similarly, the device presented in this study also includes short-circuit protection. Additionally, it features signal recording, like Keysight-6811B and Calmet C300, yet it stands out as a cost-effective alternative. Unlike available instruments with closed architecture, the proposed PQD generator offers flexibility for end-users in both hardware and software functionality. The proposed LabVIEW-based PQD generator is considered expedient in terms of

20500505, 2026, 10, Downloaded from https://scijournals.onlinelibrary.wiley.com/doi/10.1002/ese3.70602 by Sheffield Hallam University, Wiley Online Library on [14/10/2026]. See the Terms and Conditions (https://onlinelibrary.wiley.com/terms-and-conditions) on Wiley Online Library for rules of use; OA articles are governed by the applicable Creative Commons License

TABLE 7 | Measurement results and uncertainty without harmonic distortion – PQD generator frequency values.

(For 50 Hz, 1 kHz, 2.5 kHz)			
Frequency (Hz)	**50**	**1000**	**2500**
No of measurements			
1	49.9998	999.9997	2499.9998
2	49.9999	999.9998	2500.0002
3	50	1000	2500.0003
4	50	1000	2499.9996
5	50	999.9959	2499.9999
6	49.9998	999.9997	2499.9997
7	50	1000	2500.0003
8	49.9998	1000	2499.9999
9	50	999.9995	2500.0001
10	50	1000	2499.9996
Uncertainty calculation			
ST. DEV	9E-05	0.001198499	0.000257682
ST. DEV/$\sqrt{n}$	2.84605E-05	0.000378999	8.14862E-05
$f_{average}$ *(Hz)*	49.99993	999.99946	2499.99994
f_Uncertainty	3E-05	0.0003995	8.5894E-05

TABLE 8 | Measurement results and uncertainty with 5% harmonic distortion – PQD generator frequency values.

(For 50 Hz, 1 kHz, and 2.5 kHz)			
Frequency (Hz)	**50 Hz**	**1 kHz**	**2.5 kHz**
No of measurements			
1	50	999.9847	2499.9913
2	49.9969	999.9965	2499.9017
3	49.9988	999.995	2499.9975
4	50	999.9947	2499.9908
5	49.9999	999.9978	2499.996
6	50	999.9975	2499.9998
7	49.9955	999.9995	2499.9697
8	50	999.938	2499.9932
9	50	999.9991	2499.9906
10	50	999.999	2499.9948
Uncertainty calculation			
ST. DEV	0.001529	0.017866886	0.028065502
ST. DEV/$\sqrt{n}$	0.000484	0.005650005	0.008875091
$f_{average}$ *(Hz)*	49.99911	999.99018	2499.98254
f_Uncertainty	0.00051	0.00595563	0.009355167

hardware and software functionality. The portability of the proposed generator, coupled with its flexible architecture, allows for easy upgrades to a three-phase solution. This makes it well-suited for laboratory and research applications. Another factor that makes the PQD generator beneficial is the frequency range of generated voltage signals spanning from DC to 1 kHz. The proposed PQD generator offers a cost-effective solution compared to the above-mentioned power quality instruments. This device provides affordability with rich functionality, making it an attractive option for users seeking reliable power quality monitoring system without the premium cost.

Typically, PQ monitoring and disturbance classification systems are implemented on embedded controller-based hardware. Therefore, researchers often need to step down the utility voltage to the levels compatible with analog channel of embedded controller, while implementing and testing their designed PQD detection and classification algorithms. The PQD generator, with a maximum voltage

20500505, 2026, 10, Downloaded from https://scijournals.onlinelibrary.wiley.com/doi/10.1002/ese3.70602 by Sheffield Hallam University, Wiley Online Library on [14/10/2026]. See the Terms and Conditions (https://onlinelibrary.wiley.com/terms-and-conditions) on Wiley Online Library for rules of use; OA articles are governed by the applicable Creative Commons License

TABLE 9 | Measurement results and uncertainty with 10% harmonic distortion – PQD generator frequency values (For 50 Hz, 1 kHz, and 2.5 kHz).

Frequency (Hz)	50 Hz	1 kHz	2.5 kHz
No of measurements			
1	49.9999	999.9878	2499.9779
2	49.9993	999.9998	2499.997
3	49.9996	999.9972	2499.9973
4	49.9998	999.9801	2499.9997
5	50	999.9549	2499.9117
6	50	999.9472	2499.99
7	49.9993	999.9999	2499.9989
8	49.9996	999.9987	2499.9352
9	49.9998	999.9938	2499.9994
10	49.9998	999.9936	2499.9977
Uncertainty calculation			
ST. DEV	0.000242693	0.018151529	0.029660202
ST. DEV/$\sqrt{n}$	7.67463E-05	0.005740017	0.00937938
$f_{average}$ *(Hz)*	49.99971	999.9853	2499.98048
f_Uncertainty	8.08977E-05	0.00605051	0.009886734

TABLE 10 | Measurement results and uncertainty with 15% harmonic distortion – PQD generator frequency values.

(For 50 Hz, 1 kHz, and 2.5 kHz)			
Frequency (Hz)	**50 Hz**	**1 kHz**	**2.5 kHz**
No of measurements			
1	49.9999	999.9993	2499.9995
2	49.9996	999.9764	2499.9978
3	49.9999	999.9996	2499.9997
4	50	999.9957	2499.9997
5	49.9999	999.9998	2499.999
6	49.999	999.9748	2499.9997
7	50	999.9424	2499.9991
8	49.9986	999.999	2499.9996
9	50	999.9998	2499.9993
10	49.9997	999.9961	2499.9997
Uncertainty calculation			
ST. DEV	0.000457	0.01781558	0.00056116
ST. DEV/$\sqrt{n}$	0.000144	0.00563378	0.000177454
$f_{average}$ *(Hz)*	49.99966	999.98829	2499.99931
f_Uncertainty	0.00015	0.0059385	0.000187053

generation capability of ±10 V, meets laboratory and research requirements for testing such algorithms programmed on embedded controllers. However, for future work, interfacing a power amplifier with the proposed PQD generator to extend its voltage range up to utility voltage levels is a consideration.

6 | Usability Demonstration of PQD Generator Data Set With Expert Power Quality Recognition System (XPQRS)

To further illustrate the functionality and effectiveness of the proposed device, a database was created using the generator, and simulation-based investigations were conducted to demonstrate its utilization and validation. For that purpose, 15 types of PQD voltage signals with 10 cycle length were generated using the proposed generator and a data set comprising 7500 signals was acquired. The sampling rate and power frequency of 5 kHz and 50 Hz, respectively, were fixed/adjusted using the general parameter setting control-panel of the generator. Another setting related to a particular PQD signal was made using the respective control panel. Table 12 presents the details of this data set, including class label, PQD signal type, and number of waveforms generated of each class. The simulations use the XPQRS, a disturbance classification algorithm presented in a recent study for the authentication of the data set [7]. PQD signals from the acquired data set are fed to the classification system and pre-processed using the first four derivatives namely $D^{(1)}$, $D^{(2)}$, $D^{(3)}$, and $D^{(4)}$. Then, three distinguished features, Log Energy (LE), Shannon Energy (SE), and Mobility (Mob) are extracted from the raw voltage signal as well as from the derivative signals. These feature values are given as input to support vector machine classifier with quadratic kernel (QSVM) which recognizes the 15 PQ disturbances [7].

The performance of XPQRS against the PQD generator data set is assessed using standard statistical metrics of accuracy, sensitivity, and specificity. In the investigation process, 10-fold cross-validation method was employed for training and testing each classifier. Figure 15 presents a 15 × 15 confusion matrix showing the percentage accuracy results of XPQRS against the voltage-signal data set produced by the

20500505, 2026, 10, Downloaded from https://scijournals.onlinelibrary.wiley.com/doi/10.1002/ese3.70602 by Sheffield Hallam University, Wiley Online Library on [14/10/2026]. See the Terms and Conditions (https://onlinelibrary.wiley.com/terms-and-conditions) on Wiley Online Library for rules of use; OA articles are governed by the applicable Creative Commons License

TABLE 11 | Comparison of different types of power quality disturbance generator with LabVIEW-based PQD generator.

Parameters	Keysight-6811B	Calmet C300	Metrel M12191	Proposed PQD generator
Voltage uncertainty	±0.645 V	±0.046 V	±21.5 V	$\pm 10.2 \times 10^{-5}$ V
Frequency uncertainty	±5 mHz	±2.5 mHz	No information	30 uHz
Short circuit protection	YES	YES	YES	YES
PQDs	All According EN50160 and EN 61000-4 standard series	All According EN50160 and EN 61000-4 standard series	All according EN 61010-1	15 types of PQ disturbances, All according to IEEE standard 1159
Number of phases	Single	Three	Single	Single/extendable to three Phase
Hardware functionality	Standalone with PC support	PC-based	Standalone with PC support	PC-based
Software functionality	Dedicated software with closed architecture	Dedicated software with closed architecture	RS232 communication interface support	Open-source LabVIEW Software based architecture
Portability	Limited Portability	Stationary	Portable	Portable
Test signals recording	Yes	Yes	No	Yes
Output voltage resolution	10 mV	1 mV	1.11 mV	5 mV
Maximum voltage (RMS)	300 V	560 V	285 V	10 V
Frequency range	45 Hz to 1 kHz	DC to 3.2 KHz	No Information	DC to 1 kHz

20500505, 2026, 10, Downloaded from https://scijournals.onlinelibrary.wiley.com/doi/10.1002/ese3.70602 by Sheffield Hallam University, Wiley Online Library on [14/10/2026]. See the Terms and Conditions (https://onlinelibrary.wiley.com/terms-and-conditions) on Wiley Online Library for rules of use; OA articles are governed by the applicable Creative Commons License

proposed PQD generator. The diagonal elements represent the correct recognition of PQD events, and other than diagonal values show the miss-predicted PQ disturbances. The overall accuracy, sensitivity, and specificity of the classifier are 92.55%, 95.80%, and 99.38%, respectively. These performance metrics of the classification system with PQD generator data set closely coincide with the efficacy results of the system with a theoretical data set (that shows an accuracy of 96.5%) presented in [7]. The slight difference in accuracy is understandable as the signals generated by the proposed PQD generator are real-world electrical voltage signals rather than ideal simulated signals. This demonstrates the authenticity and usefulness of the proposed device in laboratory for the researchers to design and test a PQ disturbance recognition algorithm. Researchers can emulate various electrical conditions which exist in an electrical environment where the PQ monitoring system will be installed. They can construct their own data set according to their need, incorporating such conditions. The PQ disturbance detection and classification algorithm that is trained and verified using such a data set will be more practical and effective while implementing in a PQ monitoring system.

TABLE 12 | Voltage signal data set obtained from PQD generator.

Class label	PQD signal type	No. of waveforms
C1	Normal	500
C2	Sag	500
C3	Swell	500
C4	Interruption	500
C5	Spike	500
C6	Oscillatory transient	500
C7	Flicker	500
C8	Harmonics	500
C9	Notch	500
C10	Flicker with Sag	500
C11	Flicker with swell	500
C12	Sag with harmonics	500
C13	Swell with harmonics	500
C14	Sag with oscillatory transient	500
C15	Swell with oscillatory transient	500
Total		7500

7 | Conclusion

In this article, LabVIEW software platform-based PQD generator is presented. The concept of virtual instrumentation is utilized for designing a reliable PQD generator. LabVIEW software is employed for producing user-defined simulated PQD signals that is converted into real-time voltage signal using MyDAQ (a data acquisition card from NI). An interactive VI for the generation of 15 types of single and multi-complex PQD events is featured in proposed instrument. A procedure suggested by ISO standard, that is, guide to the expression of uncertainty in measurement is adopted to evaluate the efficacy and reliability if the instrument. The detailed calculations of measurement uncertainty are shown. Uncertainty in RMS voltage and frequency of generated signal has been computed using different reference frequencies of 50 Hz, 1 kHz, and 2.5 kHz with nominal RMS voltages. Experimentations to measure

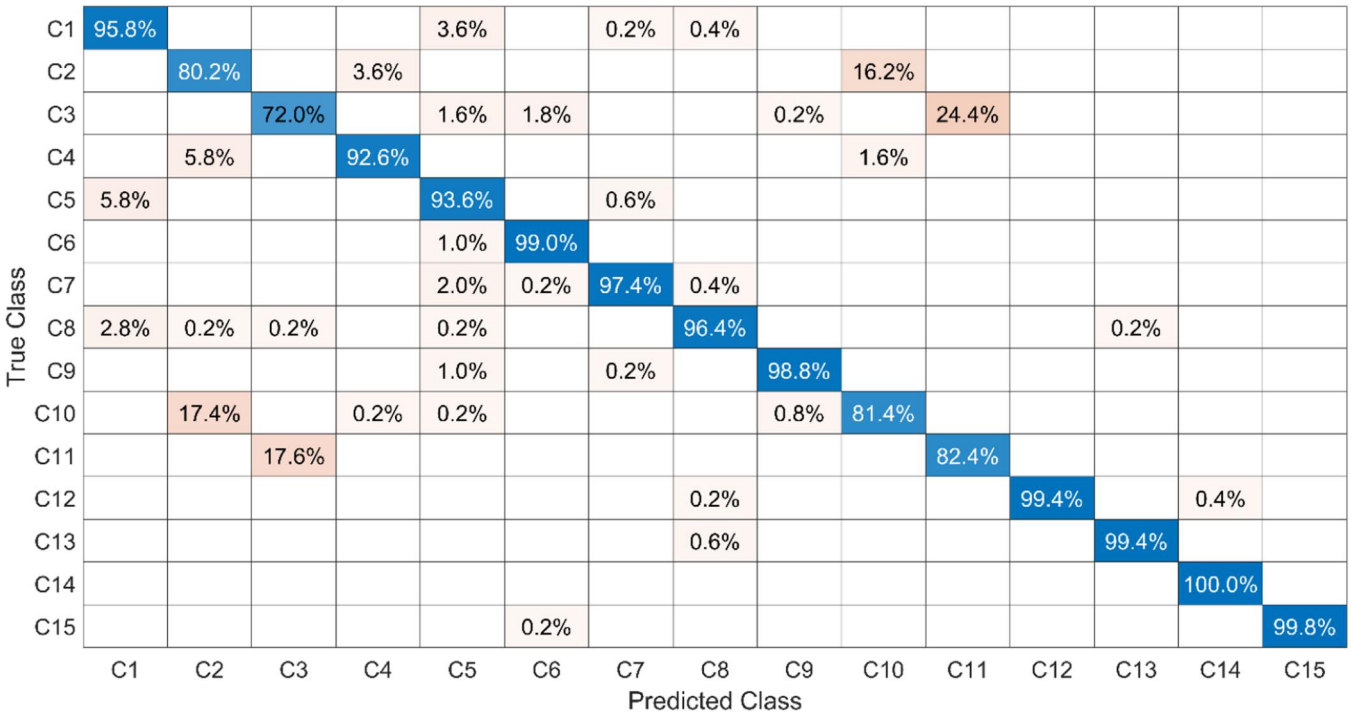

FIGURE 15 | Confusion matrix illustrating accuracy results of XPQRS against PQD generator data set.

20500505, 2026, 10, Downloaded from https://scijournals.onlinelibrary.wiley.com/doi/10.1002/ese3.70602 by Sheffield Hallam University, Wiley Online Library on [14/10/2026]. See the Terms and Conditions (https://onlinelibrary.wiley.com/terms-and-conditions) on Wiley Online Library for rules of use; OA articles are governed by the applicable Creative Commons License

the uncertainty at different harmonic distortion levels of 5%, 10%, and 15% are carried out.

The harmonic-distortion experiments show that voltage uncertainty remains below 1 mV across the tested 5%–15% THD conditions, with the worst case being 982 μV at 7.07 V RMS and 2.5 kHz. Similarly, the maximum frequency uncertainty under harmonic distortion remains below 10 mHz, with the worst case being 9.887 mHz at 2.5 kHz and 10% THD. These values confirm that harmonic distortion increases uncertainty mainly at higher frequencies, but the absolute increase remains small for laboratory-level PQD signal generation.

To further validate the authenticity of the proposed instrument, disturbance signals produced by the generator were given as input to a PQ classification system called XPQRS, presented in a recent study. The investigations revealed that XPQRS delivered approximately similar results which were presented in the relevant study that demonstrate the genuineness of the instrument. Due to simplicity and flexibility in the design, the proposed generator provides the most reliable, portable, and low-cost PQD generation method for laboratory and research related to PQ.

Future work will focus on four specific extensions of the proposed PQD generator. First, a power-amplifier stage will be interfaced with the MyDAQ output to scale the generated low-voltage waveform to utility-level voltage, enabling direct testing of power-quality instruments and protection devices under controlled laboratory conditions. This extension will require output-stage calibration, voltage-gain characterization, isolation, and overcurrent/short-circuit protection to ensure safe operation at higher voltage levels. Second, the present single-phase implementation will be extended to a three-phase PQD generation platform by synchronizing three analog output channels with controllable phase displacement, amplitude imbalance, phase-specific sag/swell, interruption, and harmonic distortion. This will allow the generator to emulate more realistic distribution-system operating conditions. Third, the generator will be upgraded using a higher-resolution and higher sampling-rate DAQ platform to improve waveform fidelity, support higher frequency transient components, and further reduce voltage and frequency uncertainty. Fourth, the number of generated PQD events will be expanded beyond the current 15 classes by including additional combined and three-phase disturbance conditions, followed by a new uncertainty evaluation under different voltage levels, frequencies, THD percentages, and SNR conditions. These extensions will strengthen the proposed generator as a flexible laboratory platform for power-quality monitoring, instrument calibration, and the practical testing of PQD detection and classification algorithms.

Author Contributions

Abdullah Saud: data curation, formal analysis, methodology, software, validation, writing – original draft, writing – review and editing. **Adil Usman:** supervision, methodology, formal analysis, resources, software, writing – review and editing, project administration. **Muhammad Umar Khan:** methodology, writing – review and editing. **Sumair Aziz:** validation, writing – review and editing. **Muhammad Faisal Nadeem:** supervision, validation, writing – review and editing. **Muhammad Akmal:** supervision, writing – review and editing.

Funding

The authors have nothing to report.

Conflicts of Interest

The authors declare no conflicts of interest.

Rights Retention Statement

For the purpose of open access, the author has applied a Creative Commons Attribution (CC BY) licence to any Author Accepted Manuscript version of this paper, arising from this submission.

Data Availability Statement

The data underlying the findings of this study can be obtained from the corresponding author upon reasonable request.

References

1. Z. Ruan, W. Hu, X. Ma, X. Xiao, L. Lei, and H. Liu, "Classification Method for Multiple Power Quality Disturbances via Label Distribution Enhancement and Multi-Granular Feature Optimization," *IET Generation, Transmission and Distribution* 17, no. 13 (2023): 3070–3083.

2. P. Kandasamy, C. Kumar, M. Lakshmanan, et al., "Initial Condition Based Real Time Classification of Power Quality Disturbance Using Deep Convolution Neural Network With Bidirectional Long Short-Term Memory," *IET Generation, Transmission and Distribution* 17, no. 23 (2023): 5135–5154.

3. F. Z. Dekhandji, A. Recioui, A. Ladada, and T. S. M. Brahim, "Detection and Classification of Power Quality Disturbances Using LSTM," *Engineering Proceedings* 29, no. 1 (2023): 2.

4. F. H. Gandoman, A. Ahmadi, A. M. Sharaf, et al., "Review of FACTS Technologies and Applications for Power Quality in Smart Grids With Renewable Energy Systems," *Renewable and Sustainable Energy Reviews* 82 (2018): 502–514.

5. R. Smolenski, P. Szczesniak, W. Drozdz, and L. Kasperski, "Advanced Metering Infrastructure and Energy Storage for Location and Mitigation of Power Quality Disturbances in the Utility Grid With High Penetration of Renewables," *Renewable and Sustainable Energy Reviews* 157 (2022): 111988.

6. M. Bajaj and A. K. Singh, "Grid Integrated Renewable DG Systems: A Review of Power Quality Challenges and State-Of-The-Art Mitigation Techniques," *International Journal of Energy Research* 44, no. 1 (2020): 26–69.

7. M. U. Khan, S. Aziz, and A. Usman, "XPQRS: Expert Power Quality Recognition System for Sensitive Load Applications," *Measurement* 216 (2023): 112889.

8. P. Khetarpal, N. Nagpal, H. H. Alhelou, P. Siano, and M. Al-Numay, "Noisy and Non-Stationary Power Quality Disturbance Classification Based on Adaptive Segmentation Empirical Wavelet Transform and Support Vector Machine," *Computers and Electrical Engineering* 118 (2024): 109346.

9. A. Usman and M. A. Choudhry, "An Efficient and High-Speed Disturbance Detection Algorithm Design With Emphasis on Operation of Static Transfer Switch," *Advances in Electrical and Computer Engineering* 21, no. 2 (2021): 87–98.

10. A. Usman and M. A. Choudhry, "Hardware Realization of an Innovative Disturbance Detection Algorithm for Control Strategy of Solid-State Transfer Switch," *IEEE Transactions on Industrial Electronics* 70 (2022): 9663–9671.

11. F. Z. Dekhandji, M. Douche, and N. Zebidi, "DVR and D-STATCOM Mitigation Techniques of Power Quality Effects on Induction Motors," *Algerian Journal of Signals and Systems* 2, no. 2 (2017): 110–129.

20500505, 2026, 10, Downloaded from https://scijournals.onlinelibrary.wiley.com/doi/10.1002/ese3.70602 by Sheffield Hallam University, Wiley Online Library on [14/10/2026]. See the Terms and Conditions (https://onlinelibrary.wiley.com/terms-and-conditions) on Wiley Online Library for rules of use; OA articles are governed by the applicable Creative Commons License

12. B. F. Khaldi, F. Z. Dekhandji, and A. Recioui, "Power Quality Disturbances: A Review of Detection, Classification, Optimization, and Mitigation Techniques," *Algerian Journal of Signals and Systems* 9, no. 4 (2024): 261–286.

13. T. Zhong, S. Zhang, G. Cai, and N. Huang, "Power-Quality Disturbance Recognition Based on Time-Frequency Analysis and Decision Tree," *IET Generation, Transmission and Distribution* 12, no. 18 (2018): 4153–4162.

14. K. Manimala, K. Selvi, and R. Ahila, "Optimization Techniques for Improving Power Quality Data Mining Using Wavelet Packet Based Support Vector Machine," *Neurocomputing* 77, no. 1 (2012): 36–47.

15. A. Yılmaz and G. Bayrak, "A Real-Time UWT-Based Intelligent Fault Detection Method for PV-Based Microgrids," *Electric Power Systems Research* 177 (2019): 105984.

16. A. Enshaee and P. Enshaee, "A New S-Transform-Based Method for Identification of Power Quality Disturbances," *Arabian Journal for Science and Engineering* 43, no. 6 (2018): 2817–2832.

17. F. Hanim M. Noh, M. Ab. Rahman, and M. Faizal Yaakub, "Performance of Modified S-Transform for Power Quality Disturbance Detection and Classification," *TELKOMNIKA (Telecommunication Computing Electronics and Control)* 15, no. 4 (2017): 1520–1529.

18. P. Li, T. Ma, J. Shi, and Q. Jia, "Multi-Dimensional Feature Multi-Classifier Synergetic Classification Method for Power Quality Disturbances," *Computers and Electrical Engineering* 120 (2024): 109720.

19. W. Zhaoqing, C. Yanzhao, C. Jianlei, and B. Weiyu, "Optimized Decomposition and Identification Method for Multiple Power Quality Disturbances," *IET Generation, Transmission and Distribution* 18, no. 21 (2024): 3501–3509.

20. P. N. Kumawat, D. K. Verma, and N. Zaveri, "Comparison Between Wavelet Packet Transform and M-Band Wavelet Packet Transform for Identification of Power Quality Disturbances," *Power Research* 14, no. 1 (2018): 37–45.

21. A. Shaik and A. Reddy, "Flexible Entropy Based Feature Selection and Multi Class SVM for Detection and Classification of Power Quality Disturbances," *International Journal of Intelligent Engineering and Systems* 11, no. 5 (2018): 140––151.

22. F. Ucar, O. F. Alcin, B. Dandil, and F. Ata, "Power Quality Event Detection Using a Fast Extreme Learning Machine," *Energies* 11, no. 1 (2018): 145.

23. S. J. Alqam and F. R. Zaro, "Power Quality Detection and Classification Using S-Transform and Rule-Based Decision Tree," *International Journal of Electrical and Electronic Engineering and Telecommunications* 8 (2019): 45–50.

24. W. Zhao, L. Shang, and J. Sun, "Power Quality Disturbance Classification Based on Time-Frequency Domain Multi-Feature and Decision Tree," *Protection and Control of Modern Power Systems* 4, no. 1 (2019): 27.

25. Institute of Electrical and Electronics Engineers. *IEEE Recommended Practice for Monitoring Electric Power Quality*. (IEEE Std., 1995).

26. "IEEE Recommended Practice for Monitoring Electric Power Quality." IEEE Std 1159–2019, 1995. (Revision of IEEE Std 1159-2009).

27. R. Machlev, A. Chachkes, J. Belikov, Y. Beck, and Y. Levron, "Open Source Dataset Generator for Power Quality Disturbances With Deep-Learning Reference Classifiers," *Electric Power Systems Research* 195 (2021): 107152.

28. M. Simić, Z. Kokolanski, D. Denić, V. Dimcev, D. Živanović, and D. Taskovski, "Design and Evaluation of Computer-Based Electrical Power Quality Signal Generator," *Measurement* 107 (2017): 77–88.

29. B. Velkovski and Z. Kokolanski, "A Virtual Signal Generator for Real-Time Generation of Power Quality Disturbances." *2020 XXIX International Scientific Conference Electronics (ET)* (IEEE, 2020).

30. C. B. Khadse, M. A. Chaudhari, and V. B. Borghate, "A Laboratory Set-Up for Power Quality Disturbance Generator and Real Time Power Quality Monitoring." *2016 IEEE International WIE Conference on Electrical and Computer Engineering (WIECON-ECE)* (IEEE, 2016).

31. P. D. Achlerkar, S. R. Samantaray, and M. Sabarimalai Manikandan, "Variational Mode Decomposition and Decision Tree Based Detection and Classification of Power Quality Disturbances in Grid-Connected Distributed Generation System," *IEEE Transactions on Smart Grid* 9, no. 4 (2018): 3122–3132.

32. C. Chunling, Q. Huihui, Z. Wei, and W. Pengfei, "Transient Power Quality Signal Generator and Detector Platform," *Energy Procedia* 16 (2012): 1380–1385.

33. M. Simic, D. Zivanovic, and D. Denic, "Development of the Signal Generator Applied to Testing of Instruments for Electrical Power Quality Measurement," *Facta Universitatis-Series: Electronics and Energetics* 25, no. 3 (2012): 193–201.

34. E.-C. Nho, I.-D Kim, T.-W Chun, and H.-G Kim, "Cost-Effective Power Quality Disturbance Generator for the Performance Test of Custom Power Devices." *30th Annual Conference of IEEE Industrial Electronics Society* (IEEE, 2004. IECON 2004).

35. N. Ullah, M. Idrees, and N. Khan, *Design and Fabrication of LV Sag/Swell Generator for CBEMA/ITI Compliance Testing* (IJSER, 2016).

36. I. J. Gabe, H. A. Gründling, and H. Pinheiro, "Design of a Voltage Sag Generator Based on Impedance Switching." *IECON 2011-37th Annual Conference of the IEEE Industrial Electronics Society* (IEEE, 2011).

37. H. Liu, F. Hussain, Y. Shen, S. Arif, A. Nazir, and M. Abubakar, "Complex Power Quality Disturbances Classification via Curvelet Transform and Deep Learning," *Electric Power Systems Research* 163 (2018): 1–9.

38. A. Usman and M. A. Choudhry, "A Precision Detection Technique for Power Disturbance in Electrical System," *Electrical Engineering* 104, no. 2 (2022): 781–796.

39. O. Zyabkina, M. Domagk, J. Meyer, et al., "Detection and Characterisation of Atypical Harmonic Patterns in Big Power Quality Data," *IET Generation, Transmission and Distribution* 19, no. 1 (2025): e70062.

40. S. A. Qureshi, M. Akmal, and R. Arif, "Power Quality Based Comparison of Compact Fluorescent Lamp with Fluorescent Light," in *2009 Third International Conference on Electrical Engineering*. IEEE, 2009), 1–6.

41. R. A. Jabbar, M. Akmal, M. Junaid, and M. A. Masood, "Operational and Economic Impacts of Distorted Current Drawn by Modern Induction Furnaces." *2008 Australasian Universities Power Engineering Conference* (IEEE, 2008), 1–6.

42. M. Désenfant and M. Priel, "Road Map for Measurement Uncertainty Evaluation," *Measurement* 39, no. 9 (2006): 841–848.

43. I. Iso and B. Oiml, *Guide to the Expression of Uncertainty in Measurement*. (International Organization for Standardization (ISO), 1995), 16–17. 122.

44. KEYSIGHT. "6811B AC Power Analyzer." 2000-2024 [23 July 2024], https://www.keysight.com/us/en/product/6811B/performance-ac-power-source-375-va-300-v-325-a.html.

45. CALMET. "C300B—Three Phase Power Calibrator and Tester." [23 July 2024], https://www.calmet.com.pl/en/c300b-three-phase-power-calibrator-features.

46. METREL. "Metrel M12191 Power Quality Analyser." [23 July 2024], https://www.metrel.si/en/.

20500505, 2026, 10, Downloaded from https://scijournals.onlinelibrary.wiley.com/doi/10.1002/ese3.70602 by Sheffield Hallam University, Wiley Online Library on [14/10/2026]. See the Terms and Conditions (https://onlinelibrary.wiley.com/terms-and-conditions) on Wiley Online Library for rules of use; OA articles are governed by the applicable Creative Commons License